A Computational Investigation of Cyclic Four-Membered Boron Based Systems

Pratip Chakraborty

A dissertation submitted for the partial fulfilment of BS-MS dual degree in Science

Indian Institute of Science Education and Research Mohali

April 2015

Certificate of Examination

This is to certify that the dissertation titled "**A Computational Investigation of Cyclic Four-Membered Boron Based Systems**" submitted by **Mr. Pratip Chakraborty** (Reg. No. MS10006) for the partial fulfilment of BS-MS dual degree programme of the Institute, has been examined by the thesis committee duly appointed by the Institute. The committee finds the work done by the candidate satisfactory and recommends that the report be accepted.

Dr. Ramesh Ramachandran Dr. P. Balanarayan

Dr. Sanjay Singh Dr. K. R. Shamasundar
(Supervisor)

Dated: April 24, 2015

Declaration

The work presented in this dissertation has been carried out by me under the guidance of Dr. K. R. Shamasundar at the Indian Institute of Science Education and Research Mohali.

This work has not been submitted in part or in full for a degree, a diploma, or a fellowship to any other university or institute. Whenever contributions of others are involved, every effort is made to indicate this clearly, with due acknowledgement of collaborative research and discussions. This thesis is a bonafide record of original work done by me and all sources listed within have been detailed in the bibliography.

Pratip Chakraborty
(Candidate)

Dated: April 24, 2015

In my capacity as the supervisor of the candidate's project work, I certify that the above statements by the candidate are true to the best of my knowledge.

Dr. K. R. Shamasundar
(Supervisor)

Acknowledgement

I would like to take this opportunity to thank my supervisor Dr. K. R. Shamasundar for giving me the opportunity to work with him and for his guidance and support throughout the project. All the discussions I had with him made me more interested towards computational research. I would like to express my gratitude to Dr. Sanjay Singh for giving me a problem to work on and helping me throughout the project. I also want to thank Dr. Ramesh Ramachandran and Dr. P. Balanarayan for their valuable comments. I would like to thank all the faculties who have helped me during my stay at IISER Mohali. I also thank IISER Mohali for the research infrastructure and DST for the continued support in form of 'INSPIRE' fellowship.

I would like to thank research scholar, Mr. Satyam Ravi for helping and guiding me with the technical part of the project. It would not have been possible without him. I would also like to thank research scholar, Mr. Deependra Bawari for helping me to understand the synthesis part of the problem. I am grateful to Dr. Jitendra Gupta for his help in the project.

My friends, both in Mohali and in Kolkata, have always supported me continuously and for that I am grateful to all of them.

Finally, yet importantly, I would like to thank my parents, elder brother, sister-in-law and relatives for their unceasing encouragement, immense support and understanding throughout this venture.

Pratip Chakraborty

“*Your work is going to fill a large part of your life, and the only way to be truly satisfied is to do what you believe is great work. And the only way to do great work is to love what you do. If you haven't found it yet, keep looking. Don't settle. As with all matters of the heart, you'll know when you find it.***”**

-Steve Jobs

“*Science is not only a disciple of reason, but, also, one of romance and passion.***”**

-Stephen Hawking

“*We wish to find the truth, no matter where it lies. But to find the truth we need imagination and skepticism both. We will not be afraid to speculate, but we will be careful to distinguish speculation from fact.***”**

-Carl Sagan

“*Those are some of the things that molecules do, given four billion years of evolution.***”**

-Carl Sagan

List of Figures

List of Tables

Notations

r: Bond distance

a: Angle

d: Dihedral angle

STO-2G: 2 primitive Gaussian orbitals are fitted to a single Slater-type orbital (STO)

DFT: Density Functional Theory

B3LYP functional: Becke, three-parameter, Lee-Yang-Parr functional

HEDM: High Energy Density Material

VSEPR: Valance Shell Electron Pair Repulsion

cc-pVNZ basis set: These basis sets are designed such that they can converge systematically to the complete basis set limit. Here, N=D,T,Q,5,6,... etc. "cc-p" stands for correlation-consistent polarised. "V" stands for valence.

cc-pVDZ-Double Zeta

cc-pVTZ-Triple Zeta

aug-cc-pVDZ: augmented version of cc-PVDZ with added diffuse functions

aug-cc-pVTZ: augmented version of cc-PVTZ with added diffuse functions

D: Dimension

PES: Potential Energy Surface

SCF: Self Consistent Field

MO: Molecular Orbital

BFGS: Broyden–Fletcher–Goldfarb–Shanno Method

HF: Hartree-Fock theory

MP: Møller-Plesset perturbation

CI: Configuration Interaction

CISD: Configuration Interaction Singles Doubles

CCD: Coupled Cluster Doubles

CCSD: Coupled Cluster Singles Doubles

CAS: Complete Active Space

MCSCF: Multi Configuration Self Consistent Field

MRCI: Multireference Configuration Interaction

MRSDCI: Multireference Singles Doubles Configuration Interaction

CASSCF: Complete Active Space Self Consistent Field

HOMO: Highest Occupied Molecular Orbital

LUMO: Lowest Unoccupied Molecular Orbital

EA: Electron Affinity

RS2C: Second-order multireference Rayleigh Schrödinger perturbation theory with a more contracted configuration space

RCCSD: Partially spin restricted open shell coupled cluster singles doubles

Contents

Abstract

Most of the previous studies on four-membered rings of boron and nitrogen like $B_2N_2H_4$ have been concerned with their Hückel analysis and to understand their aromaticity or antiaromaticity character. Synthesis of this type of ring is still very difficult and only a few have been isolated with some sterically hindered ligands. In this project, different isomers of diazadiboretine have been examined at first. Calculations have been performed to understand the stability, frequency and ring puckering of different isomers of diazadiboretidine. The most stable conformer has been determined followed by a comparative study between HF, MP2 and CCSD and an extensive basis set study. Comparative studies with other straight chain B-N systems have also been performed and B-N bond length, charge on B and N, deviation of geometry at B from planarity and at N from pyramidalisation etc. have been analyzed thoroughly. H's bonded to B's of the most stable form of diazadiboretidine have been substituted by different electron withdrawing and electron donating groups and substitutions have even been performed in the core B_2N_2 ring to check whether in any of the systems, the geometry around B atom deviates from planarity by a large amount. All the cases have been investigated thoroughly. However, it was not possible to achieve that in any of the boron based cases until we used phosphorus based 4-membered rings. Monoanion of BH_3 have also been investigated to see whether the inclusion of an electron can distort the geometry around B and our study suggests that it is not possible. Dianion of 1,3-diazadiboretidine have been examined. Monoanion and dianion of BCl_3 have also been investigated and found to be non-planar with a large deviation from planarity, but to confirm the results of this particular case and the dianion of 1,3-diazadiboretidine, more calculations need to be performed.

Chapter 1

Introduction

1.1. Introduction to Diazadiboretidine

Synthesis of B_2N_2 type of four-membered ring is very difficult and only a few have been isolated with some sterically hindered ligands. The main purpose of this project is to find out the stability and geometry of the B_2N_2 rings and to find out if there are some substituent which can make these rings stable enough so that we can make macro cycles from that using possibly more than one of these rings and the same number of linkers. The following (Fig. 1.1) is an example of a possible macro-cycle which can be formed using ethylenediamine as a linker.

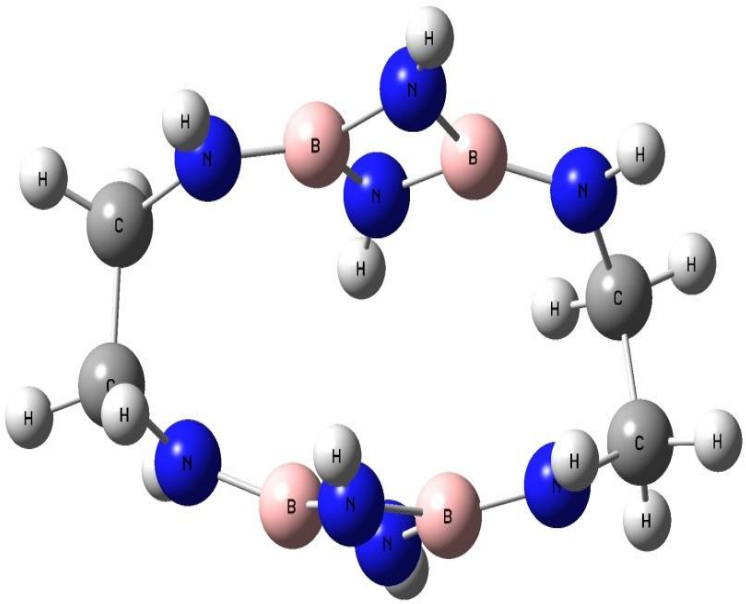

Fig. 1.1: Hypothetical macro-cycle (optimized in Gaussian09[1] using two B_2N_2 rings and two ethylenediamine (H_2N- CH_2- CH_2-NH_2) linkers)

The most important aspect to look for is to see if the substituent at B (co-ordination no. 3) bends sufficiently a large amount breaking the planar geometry around a 3-coordinated B atom, for any of the systems that we will study. It is important because it will facilitate the formation of stable macro-cycles. To study the B_2N_2 rings, we started with the simplest of these rings, different isomers of cyclo-$B_2N_2H_4$ or diazadiboretidine. It has an 1,2-conformation (Fig. 1.2) and a 1,3-conformation (Fig. 1.3) and there can be planar and puckered forms among them too which we will encounter later on.

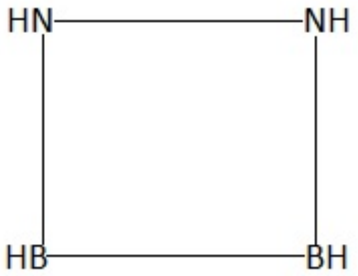

Fig. 1.2: 1,2-diazadiboretidine

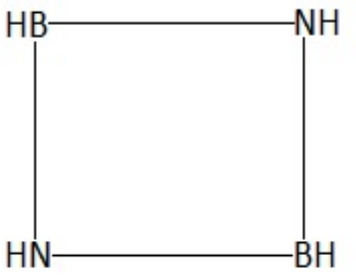

Fig. 1.3: 1,3-diazadiboretidine

1.2. Literature Survey

Most earlier work on diazadiboretidine was related to the boron-nitrogen analogue of cyclobutadiene and the level of aromaticity or antiaromaticity was an important aspect that was looked at. The synthesis of four-member rings like $B_2N_2H_4$ are in some way difficult and only a few rings with sterically hindered ligands have been isolated so far.[2]

Previously in an old study by Baird et al.[3], STO-2G calculations have been performed on the 1,3-isomer of diazadiboretidine. For the square ring, the optimum distance between B-N has been found to be 1.47 Å. For a rectangular ring using BN average separation of 1.47 Å, it have been found out that the D_{2h} form is the most stable with respect to all the displacements. These calculations also revealed that the optimum NBN angle for the D_{2h} form is 93^0 and these predictions agreed well with X-ray data.

Baird and Whitehead[4], also looked at the hückel analysis of the 1,3-isomer and compared its energy to straight chain B-N compounds and tried to understand its aromaticity.

Armstrong et al. and Baird[5] calculated the combined strain and antiaromaticity energies.

Kiran et al.[6], calculated the protonation energy of the 1,3-isomer at B3LYP/6-311G(d,p) level of theory. Their conclusion was that this isomer is antiaromatic but less so than cyclobutadiene.

Later in another study to quantify aromaticity by Rehman et al.[7], calculations revealed that the ground state structure of the 1,3-isomer of diazadiboretidine has a puckering of 17.3^0 with respect to planarity. These calculations have been done in higher level of theory - Density Functional Theory (DFT) level using B3LYP functional and 6-311G++g(d,p) basis set. The B-N bond lengths came out to be equal. The planar structure of the 1,3-isomer was also optimized and it was found out that it was 1 Kcal/mol higher in energy than the puckered structure and it had an imaginary frequency corresponding to out of plane bending mode of atoms. But this difference of energy between the two structures is comparable to thermal energy at room temperature (0.6 Kcal/mol) which suggested that the molecule could be present in both planar (although this is not actually ground state) and puckered polymorphs. A search in Cambridge Crystallographic Database also showed the presence of two crystals of these kinds. In the end, they concluded that 1,3-diazadiboretidine (puckered) is slightly aromatic, not anti aromatic.

Tricamo et al.[8] in a effort to find potential high energy density material (HEDM) optimized both 1,3-isomer and 1,2-isomer of diazadiboretidine using composite methods such as G2, G3 and complete basis set methods (CBS) and also found out their enthalpy of formation. The ground state of neither isomer has been found to be planer. 1,2-isomer was trapezoidal with a ring pucker of 5^0-7^0, B-N bond being the shortest bond among N-N,B-N and B-B, the ring angles deviating from 90^0 and hydrogen atom dihedral angles deviating from 180^0. 1,3-isomer had a ring pucker of about 20^0 and the B-N bond length was equal suggesting a delocalization of electrons. Ultimately they researched mainly about their potential as HEDM and found out that the combustion energies of these compounds are higher than other

small ringed compounds making them better HEDMs but still lesser than methane in a per gram basis.

1.3. Aim of Our Study

In this project, first of all, the equilibrium geometry and structure of cyclo-$B_2N_2H_4$ have been given the most importance. We considered verifying what previous studies[7,8] have found about different forms of diazadiboretidine. Most of the calculations have been done using single reference methods such as HF, MP2 and CCSD level of theory. After verifying and finding the most stable form of diazadiboretidine, we concentrated totally in this most stable conformation. Comparative studies have been performed by changing substituents at B atoms and also substituting atoms on the core B_2N_2 ring to see whether the planarity surrounding 3-coordinated B atom distorts by a large amount or not. In this respect, we also became interested in the anion of BH_3, anion and dianion of BCl_3 and dianion of the most stable conformation of diazadiboretidine and multireference methods have been used to investigate them. Even in these cases, our main aim was to see whether there is a large deviation from planarity around B atoms so that it can facilitate the formation of macro cycles.

Chapter 2

Theoretical and Computational Methods

A lot of geometry optimizations and frequency analysis have been done in our study using both single reference methods and multireference methods. Although, all of them are explained in detail in books [9, 10, 11], I will give a brief account of them.

2.1. Potential Energy Surface and Equilibrium Geometry

If we have a nonlinear molecule with N nuclei, its geometry is defined by 3N-6 independent nuclear coordinates which are q_1, q_2,..., q_{3N-6}. Actually, the total no of nuclear coordinates is 3N and 6 is subtracted from that as the three translational and three rotational degrees of freedom do not change E (say), the electronic energy of the molecule which is a function of these 3N-6 coordinates. This electronic energy E provides us with what we call a potential energy surface (PES) for the molecule. It is called so as E is actually the potential energy in the Schrödinger equation for nuclear motion. If E depends on two variables only, say, q_1 and q_2, then a plot of E (q_1, q_2) in 3D will provide us a surface in 3D space. Similarly, if E depends on only one variable, then a plot of E in 2D will provide us a surface in ordinary 2D space. An example of E depending on only one variable can be found in Fig. 3.20 of our study later. In reality, E depends on a large number of variables and so, it represents a surface in a higher dimensional abstract space consisting of 3N-5 dimensions. If we want to find PES of a molecule, we need to solve the electronic Schrödinger equation at many different nuclear arrangements. Calculating E for a particular nuclear configuration of the molecule gives a single-point calculation which refers to a single point on the PES of the molecule. The equilibrium geometry of a molecule corresponds to that nuclear arrangement of the molecule for which the molecular

potential energy E is minimum.

2.2. Geometry Optimization

The process of minimizing molecular potential energy E is called geometry optimization or energy minimization. There exist a lot of algorithms which can find the local minimum of a function which depends on several variables. These algorithms can find a local minimum of E in the neighbourhood of the initial geometry provided. Geometry optimizations are needed to be performed carefully. If a molecule has more than one conformation, all of them must be optimized carefully so as to locate the structure with global minimum.

2.2.1. The Computational Part

To optimize the geometry of a molecule, we start with a guess structure for the equilibrium geometry. This guess geometry that we provide is based on the typical values of bond lengths and bond angles available from earlier experimental studies or estimated from methods such as the VSEPR method. The dihedral angles that we provide are based on our experience with similar type of compounds. After providing guess geometry, one searches for the minimum nearest geometry in its neighbourhood. A basis set is chosen and SCF MO or some other method is performed to solve the electronic Schrödinger equation to get E and its gradient at that guess geometry. After that, the geometry optimization program creates a new set of values for the 3N-6 coordinates making use of the calculated E and its gradient ∇E. This new set will likely to be closer to the minimum geometry structure and the program calculates the E and ∇E at the new set of values. Again, using the calculated value of E and its gradient, another improved set is generated and SCF calculation is repeated. This process is repeated until and unless we get a value of ∇E which differs negligibly from zero (the threshold is decided beforehand and can be changed). It indicates that a minimum geometry may have been found.

2.2.2. The Theory Part

There are different algorithms to find out minimum geometry of a molecule. Some

algorithms do it by repeating calculation of potential energy E at various values of its variables to find a minimum in E, but these methods are very inefficient. However, there are more efficient procedures which make use of repeated calculation of not only E, but also its derivatives. The set of 3N-6 first partial derivatives of E with respect to its variables is what constitutes a vector which is called the gradient of E. At a local minimum, gradient has to be zero. The point on the PES where the gradient is zero is called a stationary point or a critical point. It can be a minimum, a maximum or a saddle point. Along with E and its gradient, some other procedures use the second partial derivatives of E too. These set of 3N-6 second partial derivatives of E with respect to its variables constitutes a matrix when arranged in a square array. It is called a force-constant matrix or a Hessian matrix. The Newton-Raphson method uses both first derivatives and second derivatives of E to locate a minimum of a function of several variables. There is also a modification of the Newton-Raphson method, called quasi-Newton method which instead of calculating Hessian directly, starts with a guess for the Hessian. It gradually improves this guess Hessian using the information of the calculated gradient at each step of optimization. I will explain the quasi-Newton method here as this and its modifications are the most used geometry optimization algorithm nowadays.

To explain the method, we will pretend E to be depending on only two variables X and Y which denote the guess geometry. The Taylor series for a function of two variables, neglecting terms higher than quadratic, is

$$E(X,Y) \approx E(X_1,Y_1) + \left(\frac{\partial E}{\partial X}\right)_{(X_1,Y_1)}(X-X_1) + \left(\frac{\partial E}{\partial Y}\right)_{(X_1,Y_1)}(Y-Y_1) + \frac{1}{2}.\left(\frac{\partial^2 E}{\partial X^2}\right)_{(X_1,Y_1)}(X-X_1)^2 + \left(\frac{\partial^2 E}{\partial X\,\partial Y}\right)_{(X_1,Y_1)}(X-X_1)(Y-Y_1) + \frac{1}{2}.\left(\frac{\partial^2 E}{\partial Y^2}\right)_{(X_1,Y_1)}(Y-Y_1)^2 \qquad (2.1)$$

Say,

$$E_X \equiv \frac{\partial E}{\partial X},\ E_Y \equiv \frac{\partial E}{\partial Y},\ E_{XX} \equiv \frac{\partial^2 E}{\partial X^2},\ E_{YY} \equiv \frac{\partial^2 E}{\partial Y^2},\ E_{XY} \equiv \frac{\partial^2 E}{\partial X\,\partial Y}$$

If we denote the evaluation at (X_1, Y_1) by subscript 1, the equation 2.1 becomes

$$E(X,Y) \approx E_1 + E_{X,1}(X-X_1) + E_{Y,1}(Y-Y_1) + \frac{1}{2}.E_{XX,1}(X-X_1)^2 + E_{XY,1}(X-X_1)(Y-Y_1) + \frac{1}{2}.E_{XX,1}(Y-Y_1)^2 \qquad (2.2)$$

As ab initio SCF calculation of second derivatives is very time consuming, in this

method one starts with an approximation of the Hessian and improves it as the optimization procedure proceeds. So, if we denote the first approximation to the Hessian matrix elements at or near the equilibrium geometry by superscript (1), we can write

$$E(X,Y) \approx E_1 + E_{X,1}(X - X_1) + E_{Y,1}(Y - Y_1) + \frac{1}{2}.E_{XX}^{(1)}(X - X_1)^2 + E_{XY}^{(1)}(X - X_1)(Y - Y_1) + \frac{1}{2}.E_{YY}^{(1)}(Y - Y_1)^2 \quad (2.3)$$

If we do partial differentiation of equation 2.3 with respect to X and Y, we get the following respectively.

$$E_X(X,Y) \approx E_{X,1} + E_{XX}^{(1)}(X - X_1) + E_{XY}^{(1)}(Y - Y_1) \quad (2.4)$$

$$E_Y(X,Y) \approx E_{Y,1} + E_{XY}^{(1)}(X - X_1) + E_{YY}^{(1)}(Y - Y_1) \quad (2.5)$$

$E_X(X,Y)$ and $E_Y(X,Y)$ are zero at minimum. Say, (X_a, Y_a) be the point for which the estimated first derivatives E_X and E_Y on the left sides of equations 2.4 and 2.5 are zero. Equation 2.4 becomes

$$0 = E_{X,1} + E_{XX}^{(1)}(X_a - X_1) + E_{XY}^{(1)}(Y_a - Y_1) \quad (2.6)$$

And equation 2.5 becomes

$$0 = E_{Y,1} + E_{XY}^{(1)}(X_a - X_1) + E_{YY}^{(1)}(Y_a - Y_1) \quad (2.7)$$

When we solve these two equations for X_a and Y_a, we get

$$X_a = X_1 + \frac{E_{XY}^{(1)}E_{Y,1} - E_{YY}^{(1)}E_{X,1}}{E_{XX}^{(1)}E_{YY}^{(1)} - (E_{XY}^{(1)})^2} \quad (2.8)$$

$$Y_a = Y_1 + \frac{E_{XY}^{(1)}E_{X,1} - E_{XX}^{(1)}E_{Y,1}}{E_{XX}^{(1)}E_{YY}^{(1)} - (E_{XY}^{(1)})^2} \quad (2.9)$$

We started at (X_1, Y_1) and used calculated gradient at (X_1, Y_1) and initial guess Hessian to get (X_a, Y_a). But, E is not an exact quadratic function and the Hessian matrix that we have used is just a guess Hessian and not an accurate one. So, (X_a, Y_a) is only an approximation to the point towards the minimization of E. Now, we use ab initio SCF MO for calculating E and its gradient at point (X_a, Y_a). The point (X_a, Y_a) could be used as the new starting geometry for the next cycle of optimization.

However, convergence will be faster if we use the new starting point as $X_2 = X_1 + \alpha(X_a - X_1)$, $Y_2 = Y_1 + \alpha(Y_a - Y_1)$. Here, E is expressed as a polynomial whose coefficients are determined such that E will have values that were calculated for E at (X_1, Y_1) and (X_a, Y_a) and the gradient of E will also have the calculated gradient values at (X_1, Y_1) and (X_a, Y_a). α is then varied to minimize the polynomial E which gives the new predicted geometry (X_2, Y_2) which is called a line search. We could now do a SCF calculation on E at (X_a, Y_a) and also it's gradient at that point. However, it is accurate enough to use the interpolated values of those quantities which we have found from the polynomial E fitted to the data at (X_1, Y_1) and (X_a, Y_a). Now, the estimate of Hessian needs to be improved. For that, we use the values of gradient of E at points (X_1, Y_1) and (X_2, Y_2). The improved Hessian must satisfy equations 2.4 and 2.5. We use a superscript (2) too denote the improved matrix elements. The requirement is

$$E_{X,2} = E_{X,1} + E_{XX}^{(2)} (X_2 - X_1) + E_{XY}^{(2)} (Y_2 - Y_1) \tag{2.10}$$

$$E_{Y,2} = E_{Y,1} + E_{XY}^{(2)} (X_2 - X_1) + E_{YY}^{(2)} (Y_2 - Y_1) \tag{2.11}$$

As there are 3 Hessian matrix elements and only two equations, so there is no unique solution for $E^{(2)}$. There are several procedures to find the improved $E^{(2)}$'s that satisfy equations 2.10 and 2.11 like the BFGS method. However, I will not concentrate on that. Now, we replace $E^{(1)}$'s by $E^{(2)}$'s and also (X_1, Y_1) by (X_2, Y_2) in equations 2.8 and 2.9 and calculate new coordinates. To check convergence, we see if the absolute values of the predicted coordinate changes are less than some tiny amount fixed beforehand. We do the same thing for gradients also. If these conditions are met, then the optimization is finished and (X_2, Y_2) is the predicted geometry. Otherwise, we calculate E and ∇E at the new coordinates, then do a line search like earlier to locate point (X_3, Y_3) and continue doing this until the convergence criteria is met. There are other modifications to quasi-Newton method and also some other procedures for optimizations, but they will not be discussed here further.

2.3. Molecular Vibrational Frequencies

Calculation of molecular vibrational frequencies allows one to understand if a stationary point on the PES found by geometry optimization is a local minimum or a saddle-point. When a stationary point on the PES has all real vibrational frequencies, it is a local minimum. If it has n number of imaginary frequencies, it is an nth-order saddle-point. The theoretical calculation of vibrational frequencies of a molecule is also very helpful while analyzing an infrared spectrum of that molecule. Also, by knowing molecular vibrational frequencies, one can calculate vibrational zero point energies too. Now, we know that the total energy of a molecule is approximately the sum of rotational, translational, vibrational and electronic energies of it. From the harmonic-oscillator approximation, we know that the vibrational energy (E_{vib}) of an N-atom molecule is the sum of the vibrational energies of its 3N-6 normal modes (3N-5 if it is a linear molecule). So, we can write

$$E_{vib} \approx \sum_{k=1}^{3N-6} \left(v_k + \frac{1}{2}\right) h\nu_k \tag{2.12}$$

Here, ν_k is the harmonic vibrational frequency for kth normal mode. Each of the vibrational quantum number ν_k has possible values 0,1,2,... They are independent of the values of all the other vibrational quantum numbers. As all the 3N-6 vibrational quantum numbers are zero for the ground vibrational state the zero point energy is

$$E_{ZPE} = \frac{1}{2} \sum_{k=1}^{3N-6} h\nu_k \tag{2.13}$$

To find the harmonic vibrational frequencies of a molecule, the equilibrium geometry of the molecule is taken and the second derivatives of the molecular electronic energy E are calculated at this equilibrium geometry (using the same level of theory and basis set that was used for optimization). The mass-weighted Hessian (or force constant) matrix elements are formed.

$$F_{ij} = \frac{1}{(m_i m_j)^{1/2}} \cdot \left(\frac{\partial^2 E}{\partial X_i \, \partial X_j}\right)_e \tag{2.14}$$

Here, $i, j = 1,2, \ldots, 3N$ and m_i is the mass of the atom X_i.

Next, 3N linear equations of 3N unknowns are solved. The set of equations are

$$\sum_{j=1}^{3N} \left(F_{ij} - \delta_{ij} \lambda_k\right) l_{jk} = 0 \tag{2.15}$$

Here, δ_{ij} is the Kronecker delta function. For, this set of equations to have a nontrivial solution, we need to have,

$$\det\left(F_{ij} - \delta_{ij}\lambda_k\right) = 0 \tag{2.16}$$

This determinant is of the order of 3N. When it is expanded, it gives a polynomial where the highest power of λ_k is 3N. The vibrational frequencies are then calculated from

$$\nu_k = \frac{{\lambda_k}^{1/2}}{2\pi} \tag{2.17}$$

Among the 3N values that we get, six of them will be zero which corresponds to the rotational and translational degrees of freedom of the molecule. However, in practice, as the equilibrium geometry is never found with infinite accuracy, we never get the six vibrational frequencies as zero. These values come out very close to zero and when we visualize them using some software, we can confirm that those represent rotations and translations of the molecule. The remaining 3N-6 vibrational frequencies correspond to the molecular vibrational frequencies.

2.4. Theories That Have Been Used in Our Calculations

We have performed geometry optimization of a lot of molecules. The optimizations are performed from the ab-initio principles of quantum chemistry and there are a few methods[9,10,11,12] to do that. I will explain the methods that have been used in our study qualitatively in brief in this section.

2.4.1. Single-Configuration Based Theories

Most of the widely used methods to understand geometry and energy of a molecule starts from a single configuration, mainly from a Hartree-Fock self consistent field wave function.

2.4.1.1. Hartree-Fock Theory

In this theory, the wave function Ψ_0 is a product of one electron wave functions which are referred to as molecular spin orbitals. The wave function is antisymmetric with respect to electron coordinate interchange and this is called a Slater determinant form of the wave function. The molecular spin orbitals are expanded in terms of linear combination of atom centred basis functions. In HF method, each electron moves in the average field due to all other electrons. The expansion coefficients of molecular orbitals are determined in a self consistent way. The molecular orbitals that result from this calculation are the eigen functions of Fock operator. But, HF theory is unable to take care of the correlation due to motions of different electrons. Although, the inherent antisymmetry property of this type of wave function takes care of the correlation of electron of the same spin partially, the correlation due to motions of opposite spin electrons is completely neglected in HF theory. So, HF is able to account for the most of the total energy of a molecule, but it misses out a certain component of energy which is important to understand bonding and geometry. Here come the electron correlation techniques. The electron correlation energy is defined as the difference between the exact nonrelativistic energy and the HF energy of a system. Electron correlation is required to be taken into account for the accurate understanding of molecular geometries and energies.

2.4.1.2. Perturbation Theory

Perturbation is a way to treat the electron correlation. Møller-Plesset or many body perturbation theory is the one which treats the electron correlation as a perturbation on the HF problem. In this case, the zeroth order Hamiltonian is the Fock operator which is derived from the HF wave function. In this theory, the energy and the wave function are expanded in terms of power series of the perturbation. HF energy is correct to the first order and the MP perturbations start correcting from second order. We denote corrections up to second, third, fourth ... order by MP2, MP3, MP4 ... respectively. In this theory, the correlation contributions come up though their interactions with the starting HF wave function. As the Hamiltonian contains only one and two electron integrals, only single and double excitation can contribute through direct mixing with the HF wave function in case of second and third order

energies. But, the direct mixing between single excitation and the HF wave function is not possible because of the self-consistent optimization of the HF wave function. So, second and third order energies contain contribution from only double excitations. However, for higher orders, indirect mixing is there through the double excitations. So, the fourth and fifth order energies contain contribution from single, double, triple and quadrupole excitations. Double excitations are the only contributions till the third order energies and so they are very important.

This theory is size consistent. The computational scaling increases as the order of the theory increases. So, MP2, MP3 and MP4 scale as fifth, sixth and seventh power of the size of the system. We have used MP2 method mostly as it gave a very good understanding of the systems that we have studied and also it is computationally less costly.

2.4.1.3. Configuration Interaction

One of the simplest methods to treat electron correlation is configuration interaction (CI). CI is an application of linear variational method to calculate the electronic wave function. A linear combination of different configurations or Slater determinants is used which provides a better variational solution to the exact many electron wave function. CI wave function is formed by mixing the HF wave function with single, double, triple, quadrupole ... excitations. The coefficients which determine the amount of mixing are found variationally. If all the possible excited configurations can be included in the wave function, it would give us the exact solution within the space spanned by any given basis set. This is called full configuration interaction method (FCI). However, it is not practical to use this method for many electron problems with large basis sets. Thus, truncation of configuration space is required for practical purposes which lead to limited CI methods. CISD is the most widely used CI method where only single and double excitations are taken into account and the rest are neglected. CISD method works in an iterative way. The computational dependence of each iteration of CISD scales as the sixth power of the size of the system. Still, this method has been used widely in literature. However, the major deficiency of this method is that CISD energy is not size-consistent. Many techniques have been proposed to correct the CISD energies.

Along with that other size consistent treatments such as perturbation and coupled cluster theory came up and because of them, CISD is no longer a good choice for doing calculations in the ground state. However, for excited states, CI is still a widely used technique for doing quantum chemical calculations because of its ease of definition for any state of interest.

2.4.1.4. Coupled Cluster Theory

In coupled cluster theory, first we start with an exponential form of wave function, $\Psi = e^{\hat{T}}\Psi_0$. Here, the cluster operator is $\hat{T} = \hat{T}_1 + \hat{T}_2 + \hat{T}_3 + \cdots$. This exponential form of the operator provides an efficient way to include effects of higher excitations and also keeps the size consistency of the energy. Earlier, CCD (coupled cluster doubles) was used with the wave function, $\Psi = e^{\hat{T}_2}\Psi_0$. Nowadays, CCSD method is used widely where all the single and double excitations are taken into account and the rest are neglected. The wave function for CCSD is $\Psi = e^{(\hat{T}_1+\hat{T}_2)}\Psi_0$. This method is size-consistent and within the basis set space of two electrons, it is exact. In this method, a set of projection equations (one set for the correlation energy and another set for the unknown coefficients in $\hat{T}$ operators) are solved iteratively to get the wave function and energy of the system. Triple excitations are also very important for better description of electronic structure. So, CCSDT theory has been developed which takes into account the triple excitations. However, this method has eighth-order dependence on the size of the system and so it is not practical to use it. There are other modifications of CCSDT method such as CCSDT-n and CCSD(T), which are also in use. We have used CCSD method as it is computationally less costly than CCSDT and all other modifications of it, but still gives a very good description of the structure and other properties of a system.

2.4.2. Multiconfiguration-Based Theories

All the methods that have been discussed in the last section are single-configuration based i.e. the starting HF configuration is the dominant component of the correlated wave function. In those methods, a large number of configurations with relatively small amount of contributions give rise to the correlation energies and this is called

dynamical electron correlation. But, there are certain cases where these methods will not be very useful as in those cases, starting with the HF wave function is not correct even qualitatively. There are cases where the gap between bonding and antibonding orbitals of a system may become so small that the excitations involving antibonding orbitals may become very important and to do calculations on that system starting with a single HF configuration with occupied bonding orbitals may lead to huge error. It is better to treat such systems by keeping the bonding and antibonding orbitals on an equal footing and start with a small number of configurations that arrive from that treatment. So, this type of correlation involves large contributions coming from a few orbitals and is called nondynamical electron correlation.

To treat nondynamical type of correlation, MCSCF wave functions are used. Instead of starting with a single HF configuration, here we start with a relatively small number of selected configurations. Using variational procedures, weights of these configurations are optimized along with the orbitals. MCSCF wave function gives a qualitatively correct picture in many cases where single configuration leads to a large error. However, the configurations that are selected in this method depend on one's chemical insight and understanding of the orbitals of the system of interest and that may lead to a bias in the calculation. This type of bias in selection of configurations can be removed by using CAS approach. In this approach, a set of active orbitals are selected and all possible configurations of the active electrons in that active space are taken into account in the expansion of MCSCF wave function while all of the other orbitals are kept doubly occupied or empty. If we include all electrons and orbitals in active space that will be identical to the FCI technique and that is not practical. So, orbitals are needed to be selected for active space which still depends on one's chemical insight and understanding of the orbitals.

Although, MCSCF methods take into account the nondynamical correlations, it is not adequate to describe some systems. The dynamical correlations are also needed for quantitatively correct understanding of those cases. The multireference CI is a method that has been successful in this type of cases like the treatment of excited states of molecules. In MRSDCI method, all the single and double excitations are considered with respect to a modest number of MCSCF configurations. Along with that, some other configurations exceeding a certain threshold are also considered for the final variational treatment. This method is widely used nowadays. There are other

cases, where some multireference CI procedures based on CASSCF wave function have also been used. There are even multireference perturbation theories like RS2, RS2C etc. I will not go into anymore details. Next chapter onwards, I will provide all the details of our study using the theories mentioned in this chapter.

Chapter 3

Computational Study and Analysis of Diazadiboretidine (Cyclo-$B_2N_2H_4$)

3.1. Ab initio Study on Cyclo-$B_2N_2H_4$

At first, the previous results about the most stable conformation of Cyclo-$B_2N_2H_4$ have been thoroughly verified.

3.1.1. Computational Details

1,2-diazadiboretidine(puckered) (Fig. 3.1) and 1,3-diazadiboretidine (both puckered and planar) (Fig. 3.2) have been optimized in aug-cc-pVDZ basis set. The molecules contain lone pair of electrons on nitrogen atom and to make the orbitals diffuse, the basis set aug-cc-pVDZ has been used. They have been optimized on the level of HF, MP2 and CCSD using the above mentioned basis set. Frequency calculations have also been performed for confirming the ground state equilibrium geometries. All the calculations have been performed using Molpro (Version 2012.1).[13] A comparative study between HF, MP2 and CCSD has also been done for the most stable conformation to justify using MP2 method for all the systems of this type. Another comparative study has been done between different basis sets to set aug-cc-pVDZ as benchmark for this type of systems. It has also been investigated if the most stable conformation of diazadiboretidine is really a global minimum or not.

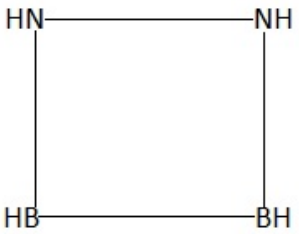

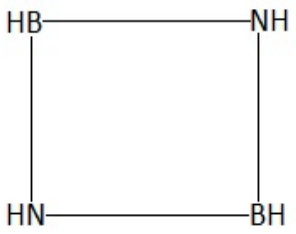

Fig. 3.1: 1,2-diazadiboretidine **Fig. 3.2:** 1,3-diazadiboretidine

3.1.2. Results and Discussion

3.1.2.1. Most Stable Conformation of Diazadiboretidine

First, we show the Z-matrix of the 1,3-isomer (both puckered and planar) in Fig. 3.3.

```
N
B  1  rBN1
N  2  rNB1  1 aNBN
B  3  rBN2  2  aBNB   1   dBNBN
H  1  rNH1  4  aHNB1  2  dHNBB
H  3  rNH2  4  aHNB2  1  dHNBN
H  4  rBH1  1  aHBN1  2  dHBNB1
H  2  rBH2  1  aHBN2  4  dHBNB2
```

Fig. 3.3: Z-matrix of 1,3-diazadiboretidine (both puckered and planar)

Fig 3.4, 3.5 and 3.6 are the optimized geometries of 1,3-diazadiboretidine (puckered) at HF, MP2 and CCSD level respectively at aug-cc-pVDZ basis set.

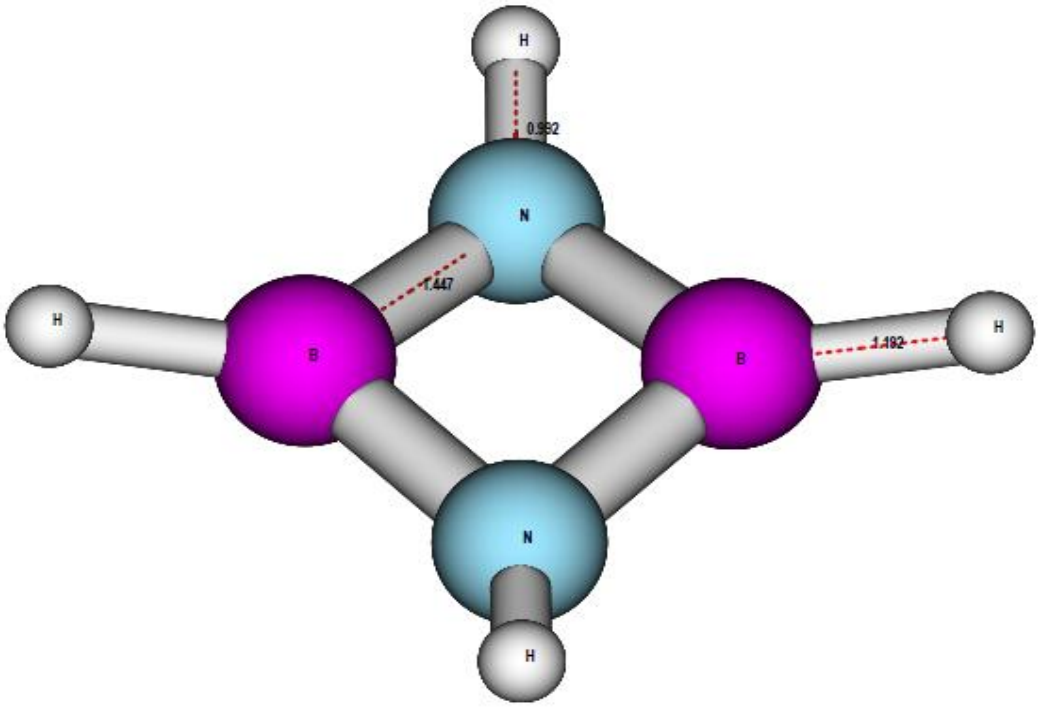

Fig 3.4: Optimized geometry of 1,3-diazadiboretidine (puckered) at HF/aug-cc-pVDZ level

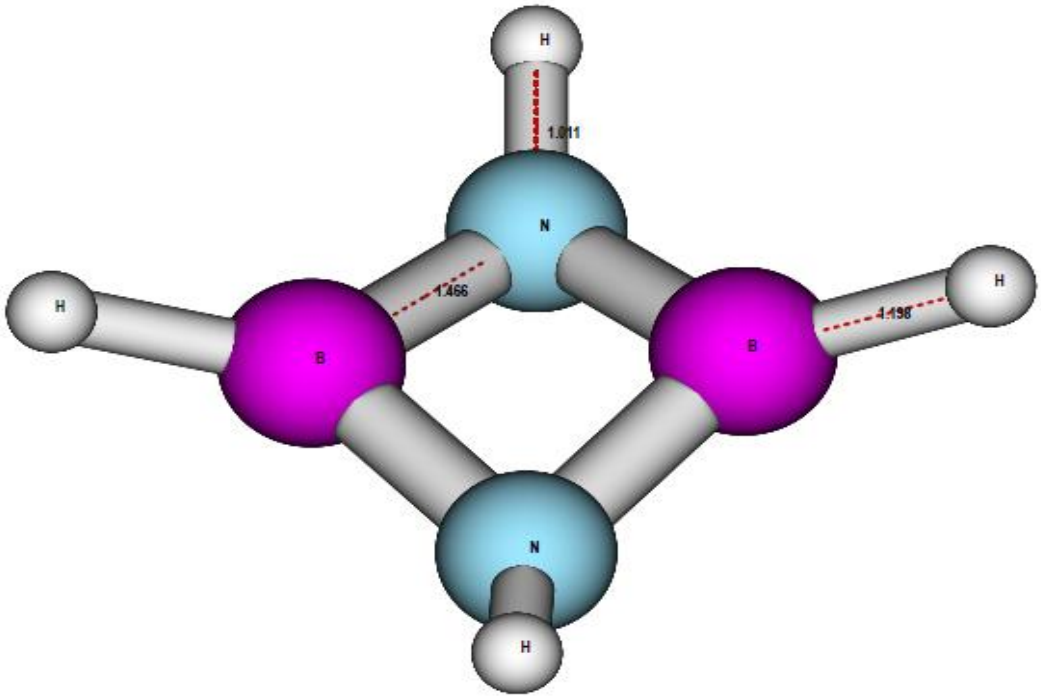

Fig 3.5: Optimized geometry of 1,3-diazadiboretidine (puckered) at MP2/aug-cc-pVDZ level

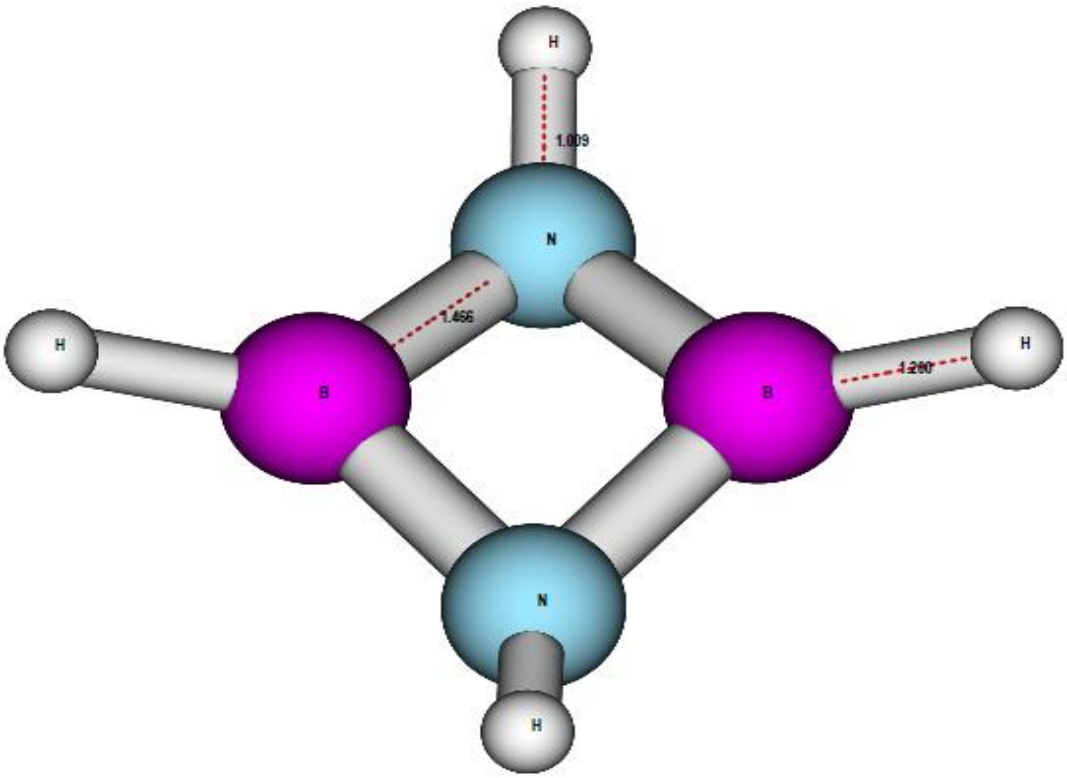

Fig 3.6: Optimized geometry of 1,3-diazadiboretidine (puckered) at CCSD/aug-cc-pVDZ level

Variable values for optimized 1,3-puckered form is given in the following Table 3.1. (All the distances are in angstroms and angles in degrees).

Table 3.1: Variable values for optimized 1,3-diazadiboretidine (puckered)

Variables	**HF**	**MP2**	**CCSD**
rBN1	1.45	1.47	1.47
rNB1	1.45	1.47	1.47
rBN2	1.45	1.47	1.47
rNH1	0.99	1.01	1.01
rNH2	0.99	1.01	1.01
rBH1	1.19	1.20	1.20
rBH2	1.19	1.20	1.20
aNBN	94.7	95.4	95.1
aBNB	85.3	81.3	82.0
aHNB1	134.6	130.8	131.2
aHNB2	134.5	130.8	131.2
aHBN1	132.6	132.0	132.2
aHBN2	132.6	132.0	132.2
dBNBN	-11.0	-19.4	-18.1
dHNBB	164.0	157.3	157.7
dHNBN	-164.0	-157.3	-157.7
dHBNB1	-164.7	-152.5	-154.1
dHBNB2	164.7	152.5	154.1

For, 1,3-diazadiboretidine (puckered), theory at all the levels reveal that the all the B-N bond lengths, all the N-H bond lengths and all the B-H bond lengths are equal. The B-N bond lengths are 1.45Å, 1.47Å and 1.47Å, N-H bond lengths are 0.99Å, 1.01Å and 1.01Å, and B-H bond lengths are 1.19Å, 1.20Å and 1.20Å at HF, MP2 and CCSD level respectively. Here the dihedral angle dBNBN represents the ring puckering (ignoring sign.). The ring puckering is almost 11.0^0 at HF level while it is 19.4^0 at MP2 level and 18.1^0 at CCSD level. So, the electron correlation does really change the ring puckering a lot and also change the bond lengths and angles by small amount. With increase in puckering in MP2 level, NBN angle increased and BNB angle decreased while again with decrease in puckering in CCSD level, NBN angle decreased slightly and BNB angle increased slightly. It can also be seen that none of the hydrogen atom dihedral angles are 180.0^0-all of them are lesser than 180.0^0 and so they are actually in one side of the ring. It is like a cis conformation. The equal B-N bond length may suggest delocalization of electrons in the ring but because of puckering it is not possible.

Fig 3.7, 3.8 and 3.9 are the optimized geometries of 1,3-diazadiboretidine (planar) at HF, MP2 and CCSD level respectively at aug-cc-pVDZ basis set.

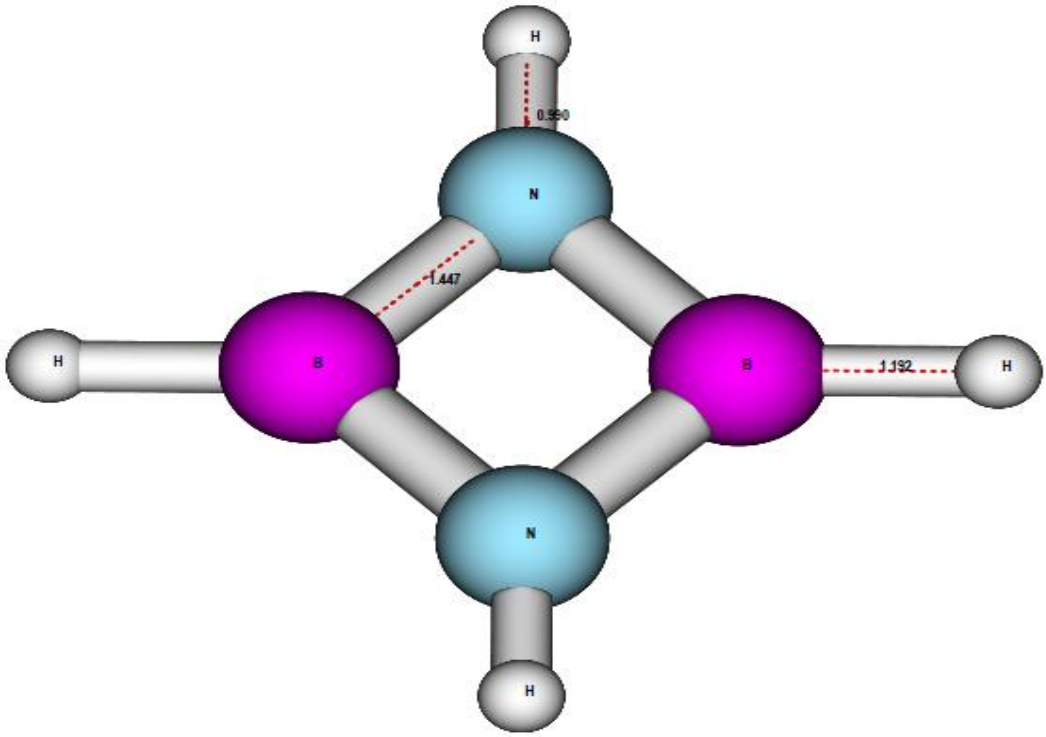

Fig 3.7: Optimized geometry of 1,3-diazadiboretidine (planar) at HF/aug-cc-pVDZ level

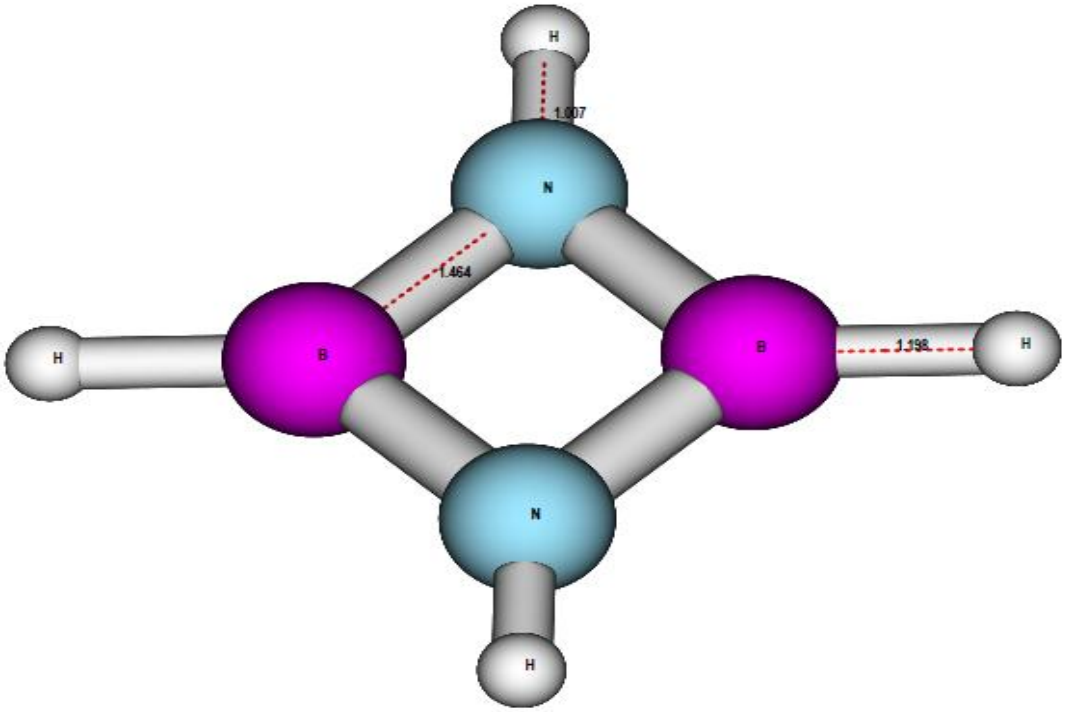

Fig 3.8: Optimized geometry of 1,3-diazadiboretidine (planar) at MP2/aug-cc-pVDZ level

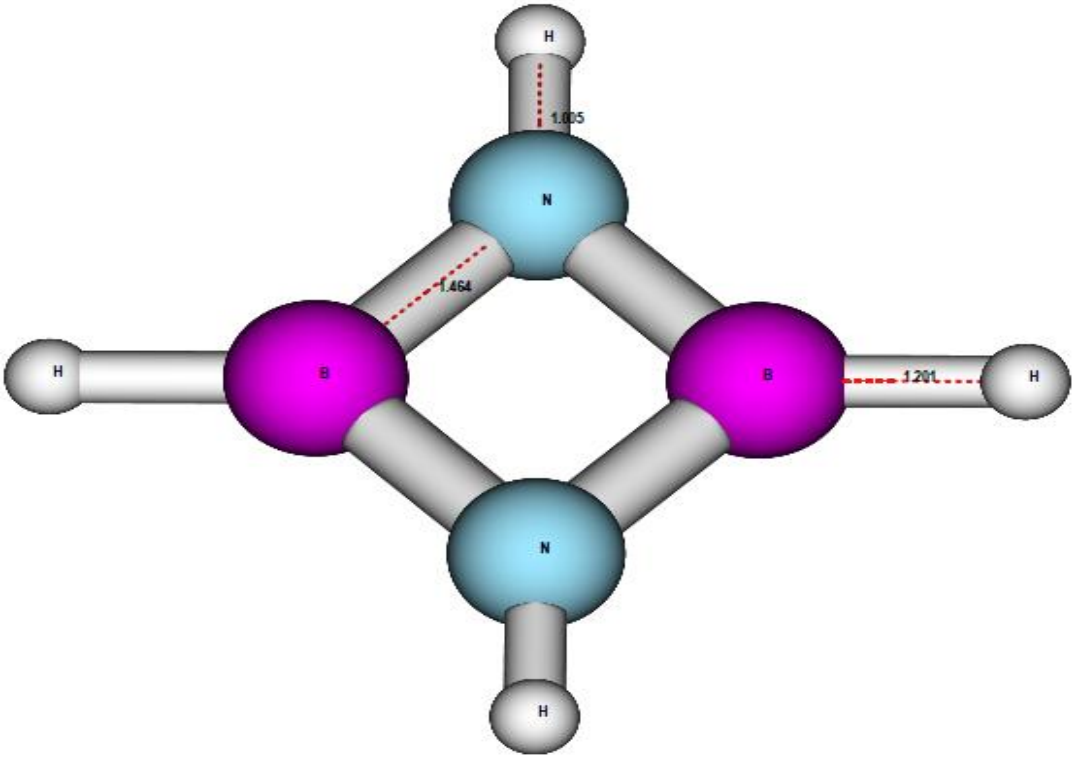

Fig 3.9: Optimized geometry of 1,3-diazadiboretidine (planar) at CCSD/aug-cc-pVDZ level

Variable values for optimized 1,3-planar form is given in the following Table 3.2. (All the distances are in angstroms and angles in degrees).

Table 3.2: Variable values for optimized 1,3-diazadiboretidine (planar)

Variables	HF	MP2	CCSD
rBN1	1.45	1.46	1.46
rNB1	1.45	1.46	1.46
rBN2	1.45	1.46	1.46
rNH1	0.99	1.01	1.00
rNH2	0.99	1.01	1.00
rBH1	1.19	1.20	1.20
rBH2	1.19	1.20	1.20
aNBN	94.3	94.6	94.4
aBNB	85.7	85.4	85.6
aHNB1	137.2	137.3	137.2
aHNB2	137.2	137.3	137.2
aHBN1	132.8	132.7	132.8
aHBN2	132.8	132.7	132.8
dBNBN	0.0	0.0	0.0
dHNBB	180.0	180.0	180.0
dHNBN	180.0	180.0	180.0
dHBNB1	180.0	180.0	180.0
dHBNB2	180.0	180.0	180.0

For, 1,3-diazadiboretidine (planar), theory at all the levels reveal that the all the B-N bond lengths, all the N-H bond lengths and all the B-H bond lengths are equal. The B-N bond lengths are 1.45Å, 1.46Å and 1.46Å, N-H bond lengths are 0.99Å, 1.01Å and 1.00Å, and B-H bond lengths are 1.19Å, 1.20Å and 1.20Å at HF, MP2 and CCSD level respectively. Here, the dihedral angle dBNBN represents the ring puckering.[7,8] Here, constrained optimizations were performed in Cs symmetry keeping dBNBN as 0^0 as we wanted the planar geometry. It can also be seen that all the hydrogen atom dihedral angles are 180.0^0 placing them in the same plane. The equal B-N bond length may suggest delocalization of electrons in the ring.

Next, we show the Z-matrix of the 1,2-conformation in Fig. 3.10.

```
N
B  1  rBN1
B  2  rBB1   1  aBBN
N  3  rBN2  2  aNBB    1  dNBBN
H  3  rBH1  4  aHBN1   1 dHBNN1
H  1  rNH1  4  aHNN1  3 dHNNB1
H  2  rBH2  1  aHBN2   4 dHBNN2
H  4  rNH2  1  aHNN2  2 dHNNB2
```

Fig. 3.10: Z-matrix of 1,2-diazadiboretidine

Fig 3.11, 3.12 and 3.13 are the optimized geometries of 1,3-diazadiboretidine (planar) at HF, MP2 and CCSD level respectively at aug-cc-pVDZ basis set.

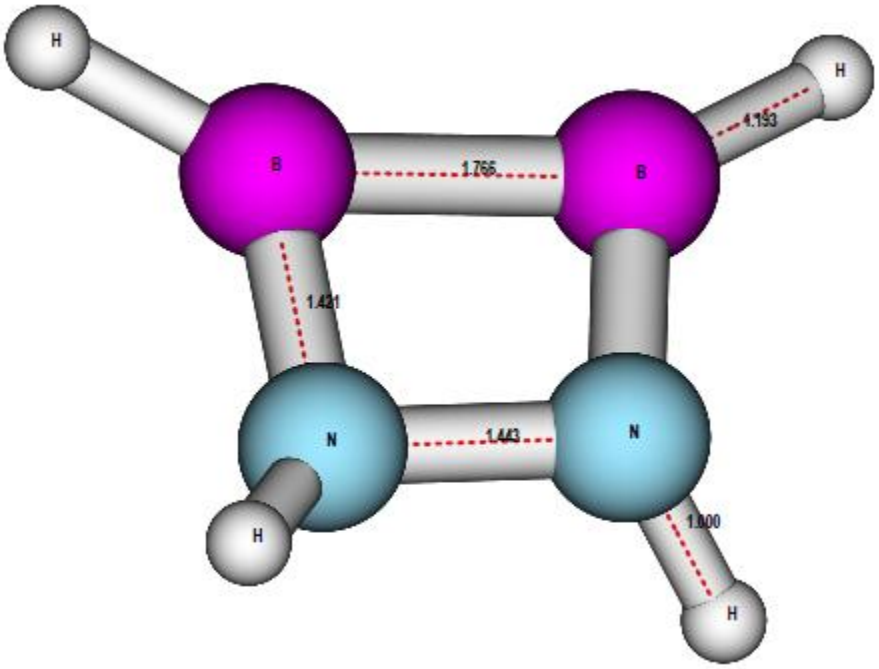

Fig. 3.11: Optimized geometry of 1,2-diazadiboretidine at HF/aug-cc-pVDZ level

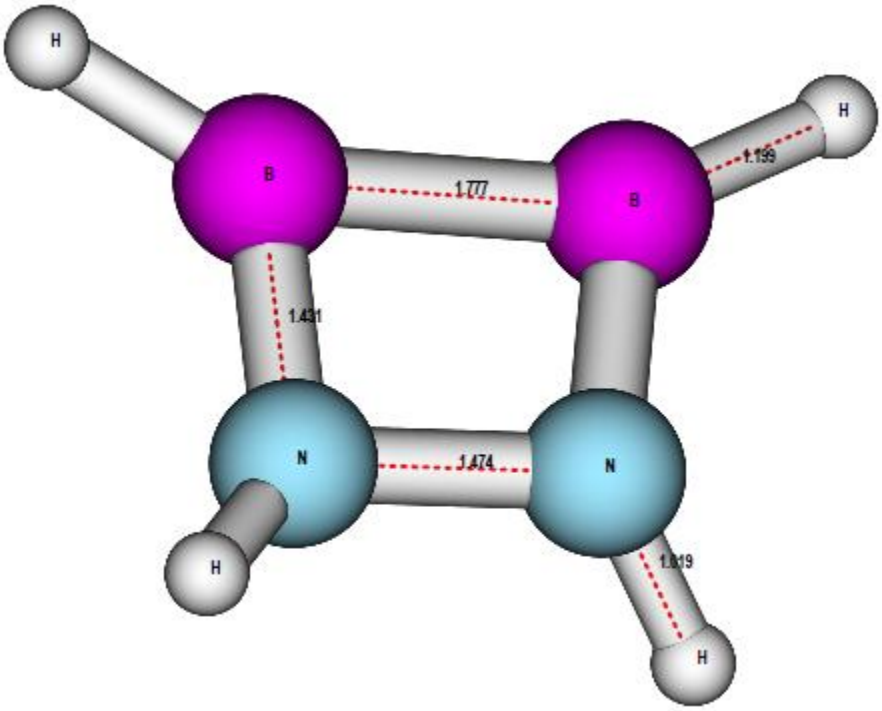

Fig. 3.12: Optimized geometry of 1,2-diazadiboretidine at MP2/aug-cc-pVDZ level

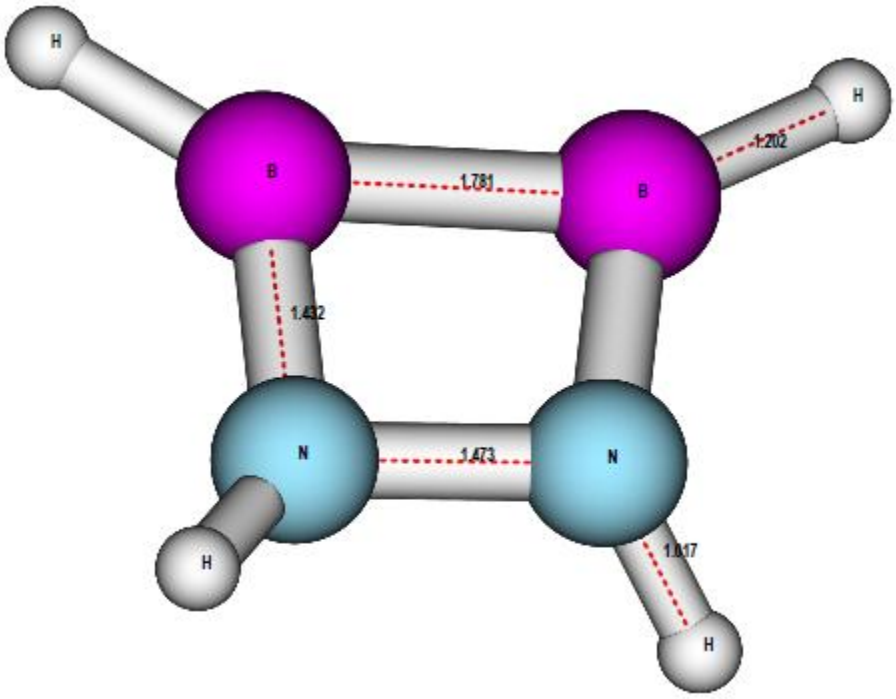

Fig. 3.13: Optimized geometry of 1,2-diazadiboretidine at CCSD/aug-cc-pVDZ level

Variable values for optimized 1,2-diazadiboretidine is given in the following Table 3.3. (All the distances are in angstroms and angles in degrees).

Table 3.3: Variable values for optimized 1,2-diazadiboretidine

Variables	HF	MP2	CCSD
rBN1	1.42	1.43	1.43
rBB1	1.77	1.78	1.78
rBN2	1.42	1.43	1.43
rBH1	1.19	1.20	1.20
rNH1	1.00	1.02	1.02
rBH2	1.19	1.20	1.20
rNH2	1.00	1.02	1.02
aBBN	83.3	83.8	83.7
aNBB	83.3	83.8	83.7
aHBN1	126.7	125.5	125.8
aHNN1	117.2	117.9	117.5
aHBN2	126.7	125.5	125.7
aHNN2	117.3	118.0	117.6
dNBBN	-6.6	-5.9	-6.2
dHBNN1	-170.6	-171.7	-171.5
dHNNB1	-149.0	-153.3	-151.8
dHBNN2	-170.5	-171.6	-171.3
dHNNB2	-149.8	-153.9	-152.4

Theory at all the levels reveals that the B-N bond lengths are smaller than N-N and B-B bond lengths. All the N-H bond lengths and all the B-H bond lengths are equal. The B-N bond lengths are 1.42Å, 1.43Å and 1.43Å, N-N bond lengths are 1.44Å, 1.47Å and 1.47Å, B-B bond lengths are 1.77Å, 1.78Å and 1.78Å, N-H bond lengths are 1.00Å, 1.02Å and 1.02Å, and B-H bond lengths are 1.19Å, 1.20Å and 1.20Å at HF, MP2 and CCSD level respectively. Here, the dihedral angle dBNBN represents the one of the four ring puckering (ignoring sign.) angles. The actual ring puckering varies in a range. None of the hydrogen atom dihedral angles are 180.0^0-all of them are lesser than 180.0^0.

The energy of the molecules, their ring puckering and presence or absence of imaginary frequency was all tabulated in the following Table 3.4.

Table 3.4: The energy, the ring puckering and presence or absence of imaginary frequency for all the conformations of diazadiboretidine

1,3-diazadiboretidine (puckered)	**Energy (Hartree)**	**HF**	**MP2**	**CCSD**
		-160.71127173	-161.22222041	-161.25202989
	Puckering Angle (degree)	10.958	19.404	18.095
	Imaginary freq. (cm^{-1})	-	-	-
1,2-diazadiboretidine (puckered)	**Energy (Hartree)**	**HF**	**MP2**	**CCSD**
		-160.56611194	-161.07882849	-161.11547367
	Puckering Angle (degree)	6.499-8.083	5.757-7.152	5.988-7.448
	Imaginary freq. (cm^{-1})	-	-	-
1,3-diazadiboretidine (planer)	**Energy (Hartree)**	**HF**	**MP2**	**CCSD**
		-160.71101030	-161.21985244	-161.25016429
	Puckering Angle (degree)	0.0	0.0	0.0
	Imaginary freq.(cm^{-1})	-129.90	-218.02	-206.73

From the optimized energy values, it can be easily seen that 1,3-diazadiboretidine puckered form is the most stable of them and the 1,2-diazadiboretidine is the least stable of them. Although, we have been able to optimize the planar conformation of 1,3-diazadiboretidine but the presence of an imaginary frequency in all levels of theory suggests that it is not a minima in the potential energy surface of the molecule (rather a maxima) while the puckered 1,3-conformation is. The ring puckering for 1,2-conformation is in a range of say,3^0 as said earlier. The Energy difference between the molecules is shown in the following Fig 3.14.

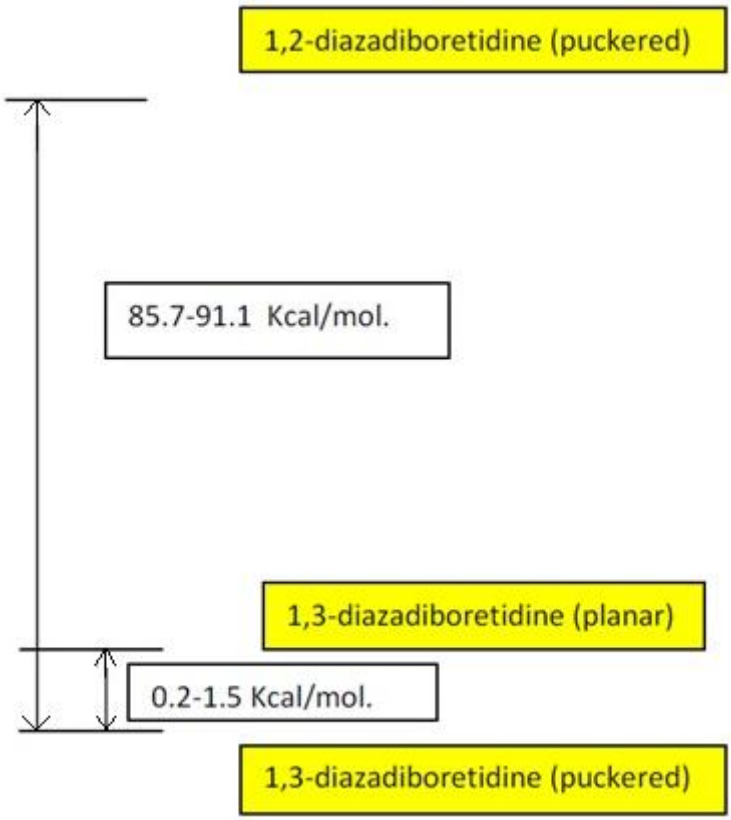

Fig. 3.14: The energy difference between the conformations of diazadiboretidine

The 1,2-conformation has a lot (approx. 90 Kcal/mol.) more energy than the 1,3 – conformations (both). So, this 1,2-diazaboretidine is not of much importance in our work. But the planer form of 1,2-diazadiboretidine is very little higher in energy than its puckered form (approx. 1 Kcal/mol.) which is very close to thermal energy at room temperature. But, the planar form is not a local minimum on the PES of the molecule as it has an imaginary frequency. So, it may be a first order saddle point on the PES.

3.1.2.2. Establishing MP2 Method for Studying 1,3-diazadiboretidine (puckered) and Similar Type of Systems

Table 3.5 shows the percentage difference for different variables of 1,3-diazadiboretidine (puckered) between HF, MP2 and CCSD methods in aug-cc-pVDZ basis set. Percentage differences have been calculated taking the variable values rounding up to sixth digit after the decimal place. However, the variable values shown here are rounded accordingly to show the difference between them.

Table 3.5: The percentage difference for different variables of 1,3-diazadiboretidine (puckered) between HF, MP2 and CCSD methods in aug-cc-pVDZ basis set

Variables	HF	%diff	MP2	%diff	CCSD
rBN(Å)	1.447	1.31	1.4664	-0.05	1.4657
rBH(Å)	1.191	0.50	1.197	0.21	1.200
rNH(Å)	0.992	1.87	1.010	-0.07	1.009
aNBN(deg)	94.7	0.75	95.4	-0.22	95.2
aBNB(deg)	84.3	-3.54	81.3	0.80	82.0
Puckering(deg)	10.958	77.08	19.404	-6.74	18.095

It can be seen that the percentage difference from HF to MP2 is a lot more than that from MP2 to CCSD for all the important variables specially the puckering angle. Introducing correlation does really change the variables a lot from HF to MP2 while the variables do not change much with introduction of another correlation i.e. from MP2 to CCSD. Also, the computational cost of CCSD is more than that of MP2. So, all the later calculations on 1,3-diazadiboretidine (puckered) or similar type of molecules will be performed using MP2 level of theory.

3.1.2.3. Establishing aug-cc-pVDZ Basis Set for Studying 1,3-diazadiboretidine (puckered) and Similar Type of Systems

Table 3.6 shows the percentage difference for different variables of 1,3-diazadiboretidine (puckered) between cc-pVDZ, aug-cc-pVDZ, cc-pVTZ and aug-cc-pVTZ basis sets at MP2 level of theory. 1,3-diazadiboretidine (puckered) has been optimized at MP2 level of theory using the above said basis sets in Gamess-US.[14] Percentage differences have been calculated taking the variable values rounding up to sixth digit after the decimal place. However, the variable values shown here are rounded accordingly to show the difference between them.

Table 3.6: The percentage difference for different variables of 1,3-diazadiboretidine (puckered) between cc-pVDZ, aug-cc-pVDZ, cc-pVTZ and aug-cc-pVTZ basis sets at MP2 level of theory

Variables	cc-pVDZ	%difference	aug-cc-pVDZ	%difference	cc-pVTZ	%difference	aug-cc-pVTZ
rBN(Å)	1.463	0.200	1.466	-0.84	1.454	0.082	1.455
rBH(Å)	1.201	-0.319	1.197	-0.946	1.1862	0.010	1.1863
rNH(Å)	1.012	-0.0012	1.010	-0.0088	1.0020	0.0005	1.0025
aNBN(deg)	95.78	-0.438	95.37	0.591	95.93	-0.230	95.71
aBNB(deg)	80.23	1.35	81.31	-0.921	80.56	0.586	81.04
dHBNN(deg)	171.39	0.323	171.95	-0.388	171.28	0.184	171.60
puckering(deg)	21.207	-8.554	19.393	-0.005	19.392	-0.938	19.21

It can be seen that the percentage difference is more mainly from cc-pVDZ to aug-cc-pVDZ and from aug-cc-pVDZ to cc-pVTZ basis sets. However, puckering is a very important aspect in this study and the percentage difference in puckering angle is most between cc-pVDZ and aug-cc-pVDZ basis sets. Also, the molecule has lone pairs on nitrogen and aug-ccpvdz basis set is computationally less costly than cc-pVTZ basis set. So, all the later calculations on 1,3-diazadiboretidine (puckered) or similar type of molecules have been performed using aug-cc-pVDZ basis set.

3.1.2.4. Concentrating on the Optimized Geometry of 1,3-puckered Conformation: Checking if it is the Global Minimum

We have provided reasons for why MP2/aug-cc-pVDZ level of theory will be used to study 1,3-diazadiboretidine (puckered) and similar type of molecules. Now, we concentrate totally on 1,3-diazadiboretidine (puckered) to see if the optimized geometry is actually a global minimum or a local minimum. If we look at the molecule carefully (Fig. 3.15), we will understand that it belongs to C_{2v} point group i.e. it has E, C_2 axis and two σ planes.

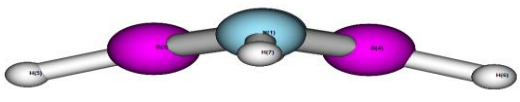

Fig. 3.15: C_{2v} symmetry of 1,3-diazadiboretidine (puckered)

So, we have considered performing the optimization in C_{2v} point group. The initial geometry that was provided is shown in Fig. 3.16. As shown, dummies have been used to form the initial geometry and when it has been optimized, it gave us the same earlier structure (Fig. 3.17). Along with that, some other optimizations have also been performed to find the global minimum. Four different initial geometries have been considered and they are as following:

1. Geometry of Fig. 3.16.
2. Both the H's attached to B in Fig. 3.17 were flipped.
3. Both the H's attached to N in Fig. 3.17 were flipped.
4. All the H's in Fig. 3.17 were flipped.

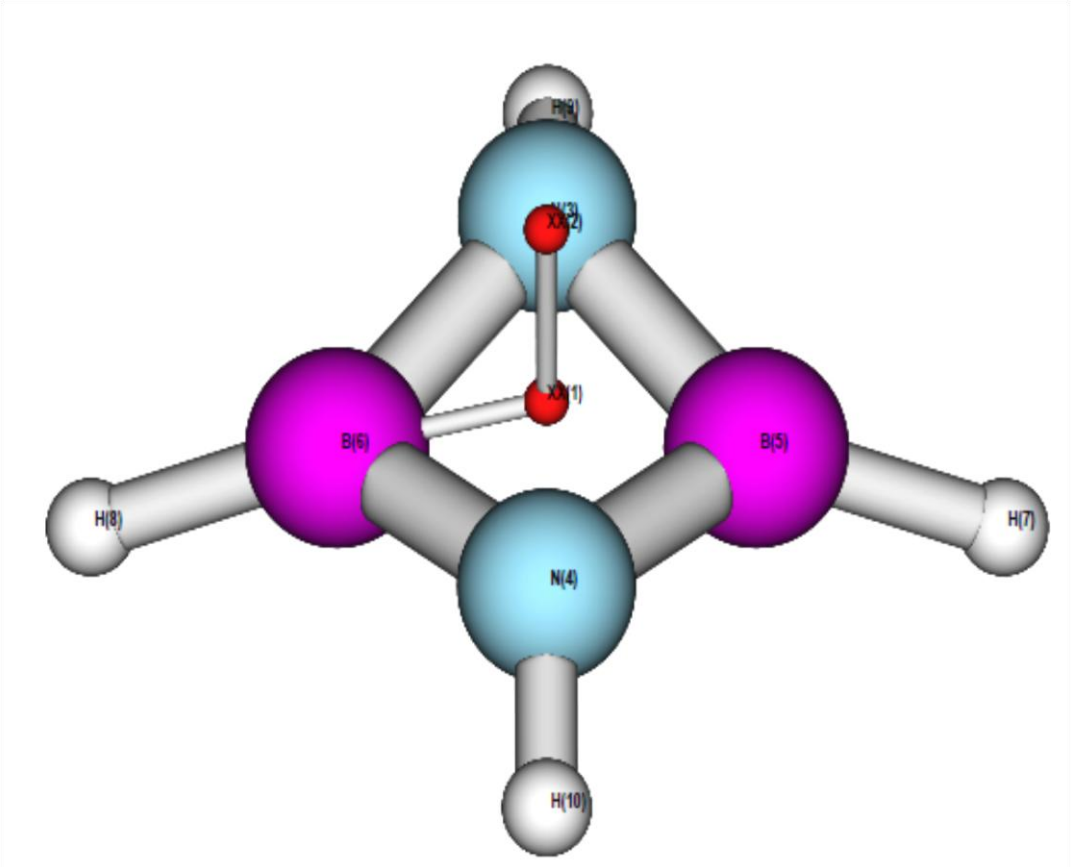

Fig. 3.16: Initial geometry using dummies to be optimized in C_{2v} symmetry

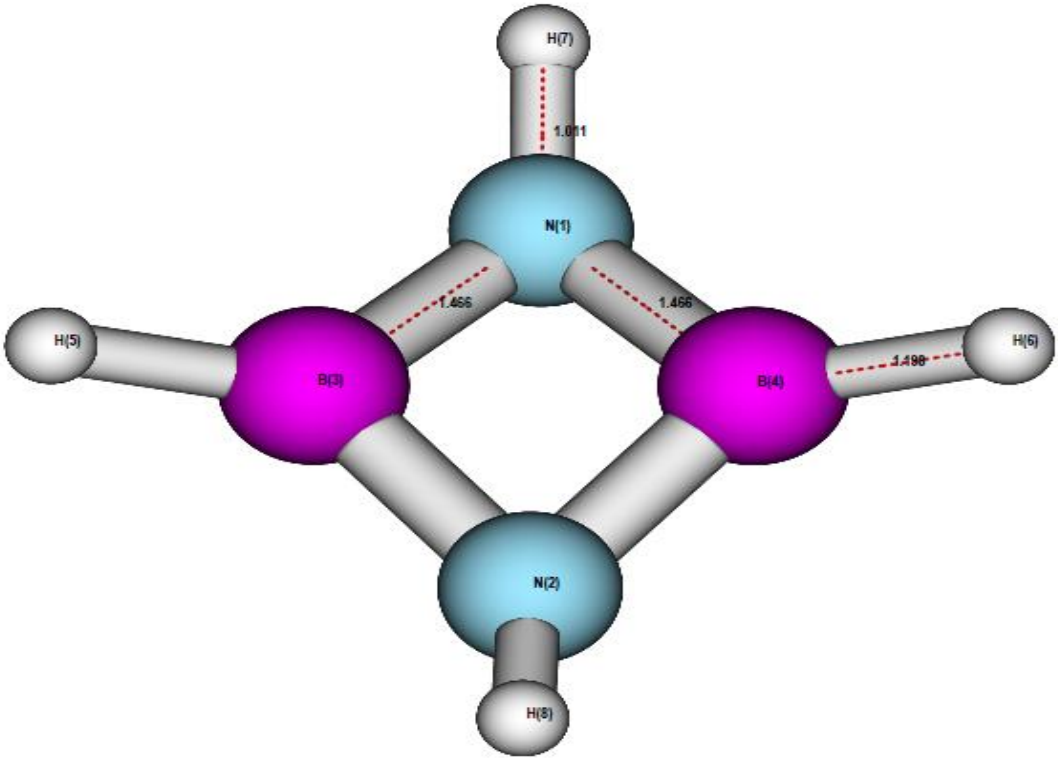

Fig. 3.17: Final optimized geometry in C_{2v} symmetry

From the optimized geometry of case (1), C_{2V} restriction was taken off and some distorted geometries (case 2-4) were optimized in C1 symmetry to confirm that the C_{2V} optimized geometry is the minimum. The energies of all the optimized geometries are shown in Table 3.17.

Table 3.7: The energies of optimized geometries of all the cases of the section 3.1.2.4

Case	E(MP2/aug-cc-pVDZ) (Hartree)
1	-161.22222**042**
2	-161.22222**038**
3	-161.22222**040**
4	-161.22222**040**

The energies of all the four cases have showed that all of them are the same structure i.e. the optimized C_{2v} structure and also none of them had any imaginary frequencies. So, it can be concluded that the C_{2v} optimized geometry is the global minimum of 1,3-diazadiboretidine (puckered).

Fig 3.18 shows the HOMO (14^{th} MO as there are total 28 electrons) and the 12^{th} MO of the molecule where we can see that the two lone pairs localized on two nitrogen atoms (there is some linear combination of one of the same symmetry lobes in case of the 12^{th} MO).

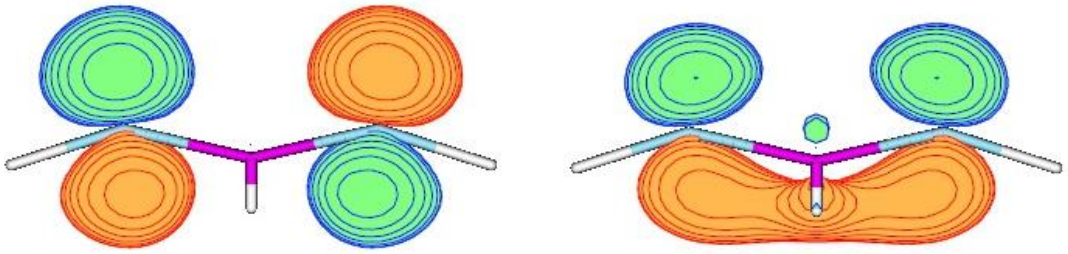

Fig 3.18: HOMO (left) and 12^{th} MO (right) of 1,3-diazadiboretidine (puckered)

The energy of the HOMO is -375392 H i.e. -10.2148 eV whereas the energy of LUMO is 0.038331 H i.e. 1.0430 eV. The energy difference between LUMO and HOMO is 11.258 eV.

Next, we considered plotting a PES with respect to puckering of the molecule. So, we defined puckering angle on our own way.

Referring to Fig. 3.19, the puckering angle = aBXX - 90^0 = θ-90^0

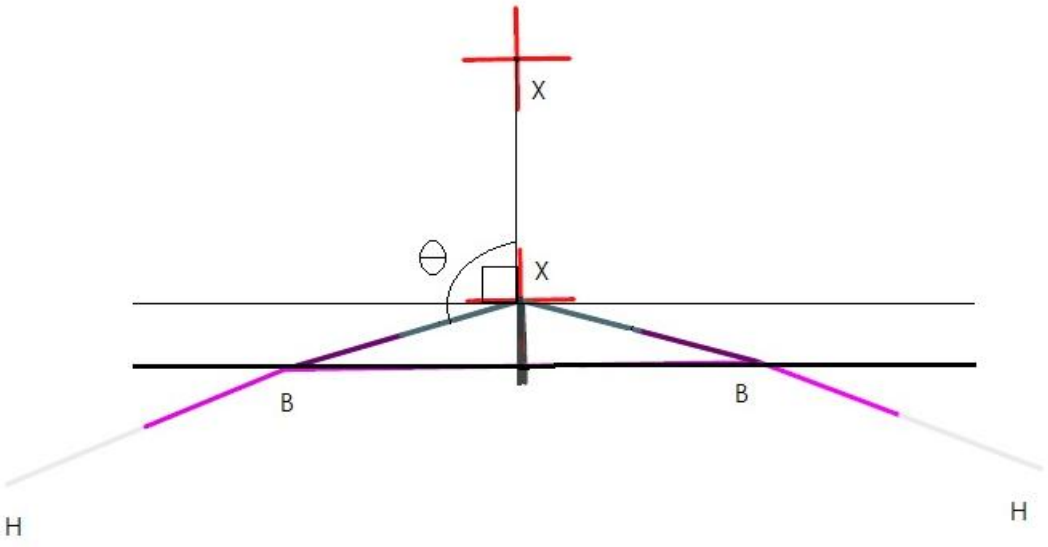

Fig. 3.19: Our definition of puckering angle in 1,3-diazadiboretidine (puckered)

We have varied the angle θ and optimized all other variables of 1,3-diazaboretidine (puckered) at MP2/aug-cc-pVDZ level. The angle θ was varied at a difference of 2^0 from -60^0 to 60^0. The energies have all been plotted with respect to the puckering angle. The minimum energy geometry was taken to be zero and all other energies have been plotted relative to that in Kcal/mol. Fig. 3.20 shows the plot of relative energy with respect to puckering angle (-30^0 to 30^0).

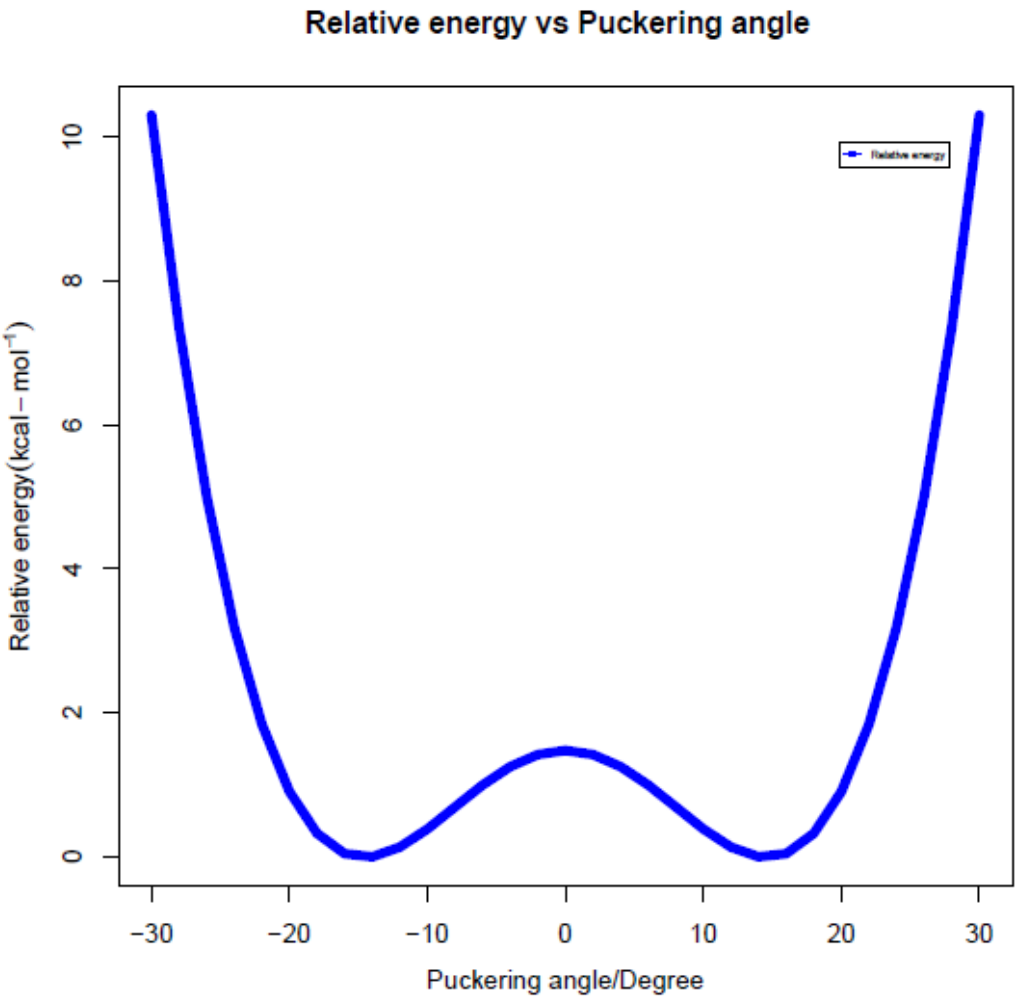

Fig. 3.20: Relative Energy vs puckering angle of 1,3-diazadiboretidine (puckered)

It can be easily seen that at -14^0 and 14^0 puckering angle, we get the global minima which have been taken as zero energy. It can be easily understood that both the structures are the same. The puckering angle for minimum energy structure in this case is not exactly the same as that of the earlier case because previously the definition of puckering was different. There exists a local maximam at 0^0 i.e. the planar conformation of 1,3-diazadiboretidine is actually a local maximum on the PES. As, the puckering angle is increased, the energy only increases and there are

no other stationary point on the PES. So, in conclusion, this plot validated all the previous studies that we have been doing on 1,3-diazadiboretidine.

Chapter 4

Analysis of Straight Chain B-N Compounds, Substituent Effect on Cyclo-B_2N_2 Rings and Effect of Substituting Atoms of the Core Ring

4.1. Straight Chain B-N Moieties: B-N Bond Distance and Mulliken Population on B and N

Before replacing other substituents in place of H's attached to B's in 1,3-diazadiboretidine (puckered), we considered some straight chain B-N moieties to understand what happens to the B-N bond distance in those moieties, the charge on B and N in them and whether they are planar or not.

4.1.1. The Computational Details

First, optimization of borane (BH_3) and ammonia (NH_3) have been performed in MP2/aug-cc-pVDZ level. As expected, optimized structure of BH_3 (Fig.4.1) came out to be planar and that of NH_3 (Fig. 4.2) came out to be pyramidal. We have replaced the H's attached to B by -NH_2 in BH_3 one by one to form BH_2-NH_2, BH-$(NH_2)_2$ and B-$(NH_2)_3$ respectively. We have also replaced the H's attached to N by -BH_2 in NH_3 one by one to form NH_2-BH_2, NH-$(BH_2)_2$ and N-$(BH_2)_3$ respectively. All of these moieties have been optimized at MP2/aug-cc-pVDZ level of theory. Along with that, the BH_3-NH_3 Lewis acid adduct has also been optimized at the same level of theory. Mulliken populations have also been found out for all the above mentioned optimized geometries at CISD/aug-cc-pVDZ level. All the calculations have been performed in Molpro (version 2012.1).[13]

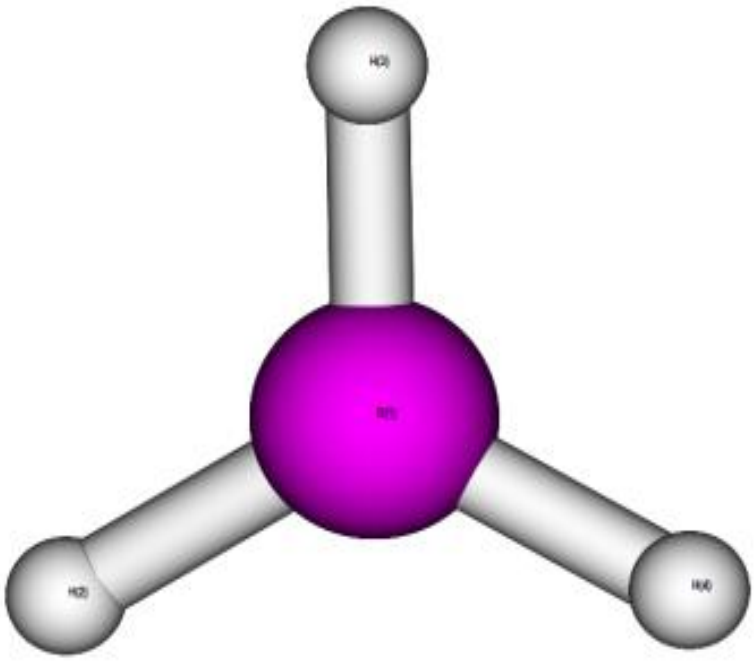

Fig. 4.1: Optimized geometry of BH_3 at MP2/aug-cc-pVDZ level

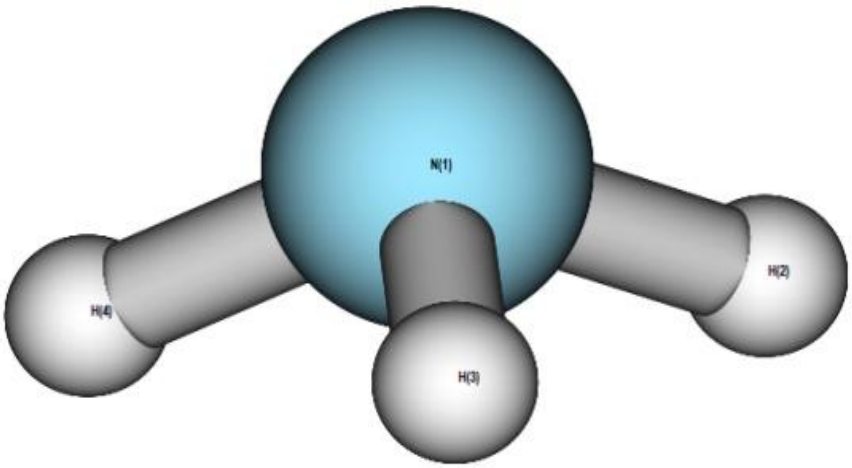

Fig. 4.2: Optimized geometry of NH_3 at MP2/aug-cc-pVDZ level

4.1.2. Results and Discussion

Fig. 4.3-4.8 shows the optimized geometry of all the above mentioned moieties.

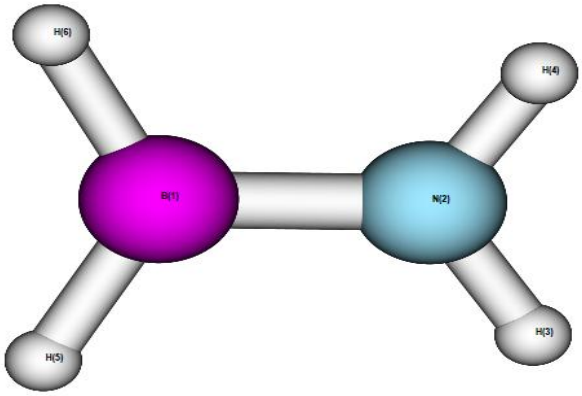

Fig. 4.3: Optimized geometry of BH_2-NH_2 (or NH_2-BH_2) at MP2/aug-cc-pVDZ level

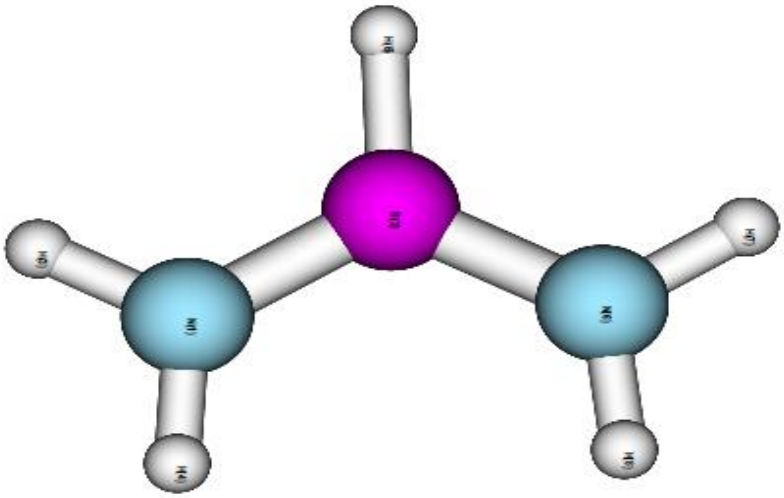

Fig. 4.4: Optimized geometry of BH-$(NH_2)_2$ at MP2/aug-cc-pVDZ level

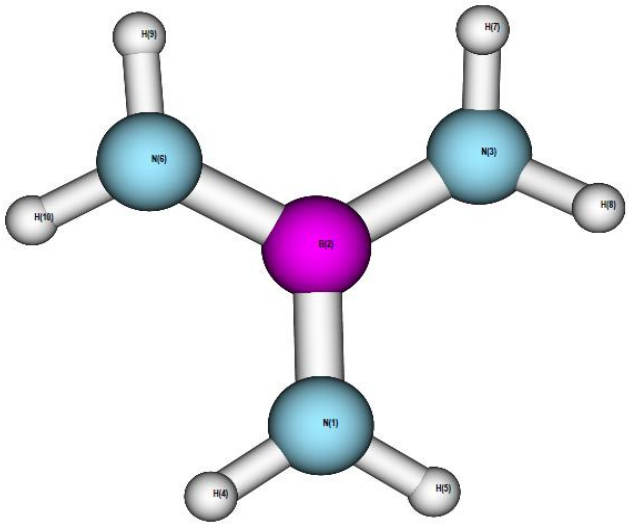

Fig. 4.5: Optimized geometry of B-$(NH_2)_3$ at MP2/aug-cc-pVDZ level

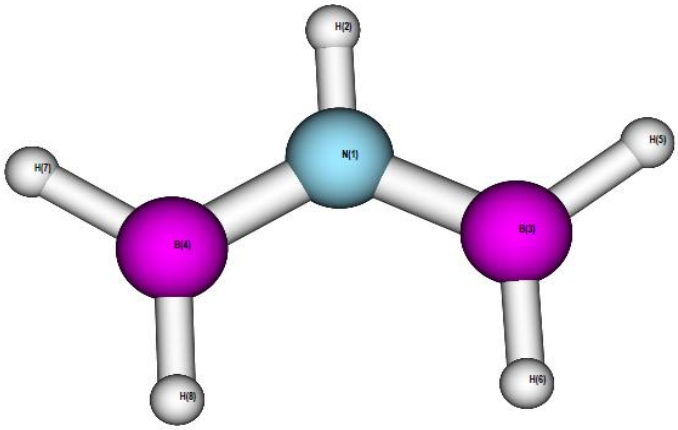

Fig. 4.6: Optimized geometry of NH-$(BH_2)_2$ at MP2/aug-cc-pVDZ level

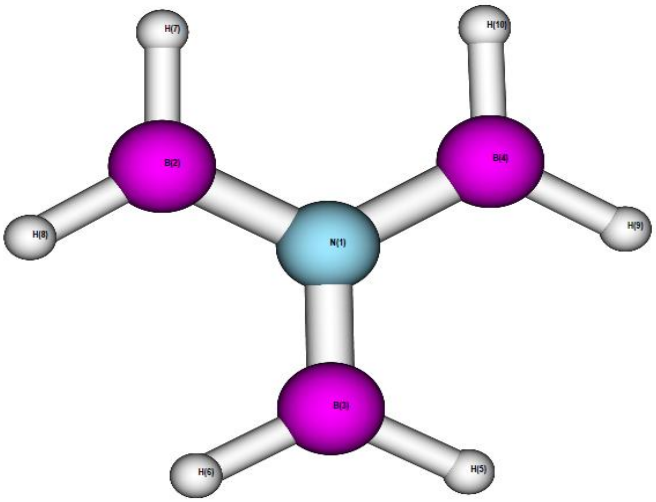

Fig. 4.7: Optimized geometry of N-$(BH_2)_3$ at MP2/aug-cc-pVDZ level

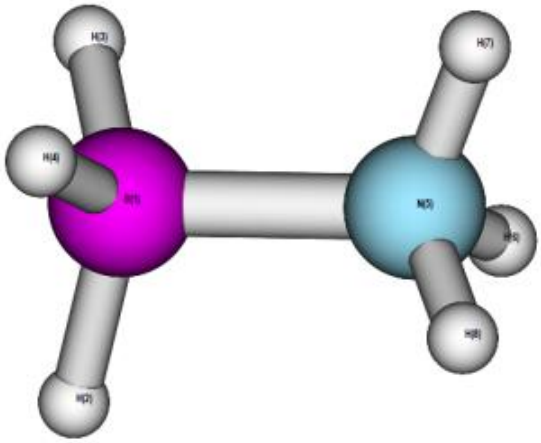

Fig. 4.8: Optimized geometry of BH_3-NH_3 Lewis acid adduct at MP2/aug-cc-pVDZ level

Table 4.1 shows all the average B-N bond lengths and the Mulliken population on B and N

Table 4.1: The average B-N bond lengths and the Mulliken population on B and N of the straight chain moieties

Moiety	Avg. BN length(Å)	Charge on B	Charge on N
BH_2-NH_2	1.404	0.027	-0.077
BH-$(NH_2)_2$	1.425	0.036	-0.160
B-$(NH_2)_3$	1.460	0.071	-0.203
BH_3-NH_3	1.668	-0.044	0.002
NH-$(BH_2)_2$	1.435	0.099	-0.025
N-$(BH_2)_3$	1.439	0.150	-0.062

We have seen that for 1,3-diazadiboretidine (puckered), the average B-N bond length is 1.466 Å. Here, we can see that for all the moieties, the average bond distance of B-N varies a lot between average B-N single bond (1.51 Å) and double bond (1.31 Å). However, it can be seen that as we have replaced H's of BH_3 by -NH_2 groups one by one, the average BN length has increased and the same has happened when we have replaced H's of NH_3 by -BH_2 groups. It is as if, that the average B-N bond length increased when the number of B-N bonds increased. There is probably some level of delocalization happening between B and N and depending on that the BN lengths are changing. Also, as we replace H's of BH_3 by -NH_2 groups one by one, charge on B increases. It is because with increasing number of -NH_2 groups, the negative charge increases in the moieties and so, the positive charge on B also increases to make it neutral. Similarly when we replace H's of NH_3 by -BH_2 groups, to counter the positive charge introduced by -BH_2 groups, the negative charge on N increases. However, a very different picture is seen for the Lewis adduct. It has a B-N bond length which is a lot larger than the average B-N single bond (1.51 Å) and double bond (1.31 Å) and it is because it actually does not have a real B-N bond as it is just an adduct where the N of NH_3 donates its lone pair of electrons completely to B of BH_3. It is because of the same reason that the charge on B is negative and the charge on N is positive in this Lewis adduct.

4.2. Substituent Effect: Average B-N length and Mulliken Population of B and N

From the optimized geometry of 1,3-diazadiboretidine (puckered), we have realized that the geometry around 3-coordinated B atom in this molecule is slightly distorted from its planar form and that is because of the B_2N_2 ring and its puckering. Albeit cis to one another, the deviation from planarity for both the H's attached to B's are very small. So, we considered replacing H's attached to B's by some other electron donating and electron withdrawing groups in order to see their effect on the geometrical parameters. Here, we have used electron donating groups such as -NH_2, -CH_3 and -SH. While -NH_2 is a strong electron donating group, -CH_3 is a weak one and -SH is very weak. -Cl and -CN were used as electron withdrawing groups and they are both very strong electron withdrawing groups (-CN is stronger among the two as –Cl is slightly electron donating). The issue of average B-N bond length and Mulliken population of B and N will be addressed in this section while the deviation from planarity and pyramidalization will be addressed in detail in section 4.3.

4.2.1. Computational Details

As mentioned earlier, we have substituted the H's attached to B's in the optimized geometry of 1,3-diazadiboretidine (puckered) by -NH_2, -CH_3, -SH, -Cl and -CN. All the new structures have been optimized at MP2/aug-cc-pVDZ level of theory. These particular calculations have been performed in Gamess-US.[14]

4.2.2. Results and Discussions

In each of the substitutions, the optimized geometry that we have gotten consists of no imaginary frequencies i.e. we have located the local minima in all the cases. Other than -NH_2, all other substitutions have led to almost the same kind of geometry as the parent molecule and so, I have not shown any figure of them. In case of -NH_2 substitution, the optimized geometry (Fig. 4.9) was almost planar. The ring puckering came out to be zero degree and the deviation from planarity was also negligible. Although, this could also be an interesting aspect to study, we have not

investigated this molecule as its planarity is not an important aspect in our study.

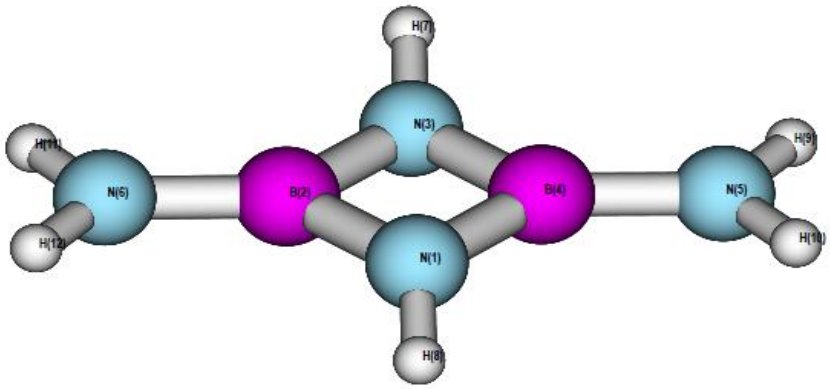

Fig. 4.9: Optimized Geometry when H's attached to B's are replaced by -NH_2 groups at MP2/aug-cc-pVDZ level

Table 4.2 shows all the average B-N bond lengths and the Mulliken population on B and N

Table 4.2: The average B-N bond lengths and the Mulliken population on B and N for the molecules formed by replacing H's attached to B's by electron donating and withdrawing groups.

Substituent on B	Avg. BN length(Å)	Charge on B	Charge on N
H	1.466	0.146	-0.179
Cl	1.457	0.213	-0.183
SH	1.465	0.172	-0.204
CH_3	1.471	0.191	-0.213
NH_2	1.473	0.128	-0.252
CN	1.460	0.325	-0.188

In all the above cases, the average B-N bond length is almost same and varies very little. However, for substitutions with electron withdrawing groups –Cl (-Cl is acting as an electron withdrawing group here) and -CN, it can be seen that the average B-N length decreases a little from that of 1,3-diazadiboretidine (puckered). Even for the electron donating groups -NH_2 and -CH_3, a small increase in the average B-N bond length than that of 1,3-diazadiboretidine (puckered) is noted. As expected from the trend, for -SH substitution, the average B-N bond length should have increased a little than that of the H substituted parent molecule but it is actually slightly lesser than that. It may be because there are some other effects involved also other than the effect of electron donation and electron withdrawal. A sharp increase of charge on B is noted for -Cl and -CN substitution from that of the parent molecule. As -Cl and –

CN withdraw electrons from their bond with B, the charge on B also increases. In a similar way, -NH_2 donates electrons in its bonding with B, and so the charge on B decreases than that of the parent molecule. However, by this logic the charge should also decrease on B for the weakly electron donating groups, -CH_3 and -SH. But, contrary to that, it can be seen that the charge on B has increased a little for -CH_3 and -SH substitution which suggests that may be some other factor is in play too.

4.3. Solid Angle as Measure of Deviation from Planarity and Pyramidalization

We know from geometry that Solid angle is the 2D angle in 3-dimensional space which an object subtends at a point. In the SI system, a dimensionless unit called a steradian (sr) is used to express a solid angle. It is a measure of how large an object appears to an observer when looking from a point. So, even a small object near a point may subtend the same solid angle as a larger object farther away at that same point. The solid angle of a sphere is defined as

$$\Omega = \frac{A}{r^2} \text{ sr} \tag{4.1}$$

For a sphere, Area,$A = 4\pi r^2$, so, $\Omega = 4\pi$ sr = 720^0

Our interest here was to quantify the deviation from planarity at B and the deviation from pyramidalization at N, for all the straight chain B-N moieties and the substituted molecules. We know that for a 3-coordinated B (say, BH_3), the stable geometry is planar and for a 3-coordinated N (say, NH_3), the stable geometry is pyramidal. So, the idea was to look for the deviation in those geometries around 3-coordinated B and N for all the moieties and molecules. Here, we have quantified the deviation by calculating the solid angle subtended at O by the area ABC (Fig 4.10).

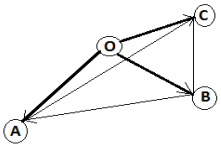

Fig. 4.10: Definition of solid angle

An efficient algorithm to measure the solid angle of this type is well known in literature[15] which have been used to write a program and calculate the necessary solid angles. The formula to calculate the solid angle Ω subtended by a triangular area ABC where $\vec{a}$, $\vec{b}$ and $\vec{c}$ are the vector positions of vertices A,B and C.

$$\tan\left(\frac{1}{2}\Omega\right) = \frac{|\vec{a}\vec{b}\vec{c}|}{abc+(\vec{a}.\vec{b})c+(\vec{a}.\vec{c})b+(\vec{b}.\vec{c})a} \qquad (4.2)$$

Here $|\vec{a}\vec{b}\vec{c}|$ denotes the determinant of the matrix which results when writing the vectors together in a row and this is also equivalent to scalar triple product of the 3 vectors.

We have calculated the solid angle of BH_3 at B subtended by the 3 H atoms which came out as 360.0^0 and that of NH_3 at N subtended by 3 H atoms which came out as 158.9^0. These two values will be our references when calculating the deviations. The deviation from planarity at B = 360.0^0 - Solid angle of the moiety/molecule at B subtended by the 3 linked atoms. The deviation from pyramidalisation at N = Solid angle of the moiety/molecule at N subtended by the 3 linked atoms – 158.9^0.

4.3.1. Straight Chain B-N Moieties: Deviation from Planarity and Pyramildalisation

Table 4.3 shows the solid angles at B and N and deviations from planarity at B and pyramidalisation at N for straight chain B-N moieties. The solid angle at B for all the straight chain B-N moieties are almost 360^0 and the deviation from planarity at B is almost negligible. The solid angles at N for all the straight chain moieties are also around 360^0. However, for B-$(NH_2)_3$, the geometry around N is slightly distorted from planarity. All of these moieties have a huge deviation from pyramidalisation around N. For the Lewis acid adduct BH_3-NH_3, the situation is quite different. The N donates its lone pair of electrons to B and in the process distorts the geometry around B. The solid angle at B becomes 219.6^0 which is more closer to a pyramidal geometry than a planar geometry. The geometry at N also deviates a little towards planarity but it is only 8.9^0.

Table 4.3: The solid angles at B and N and deviations from planarity at B and pyramidalisation at N for straight chain B-N moieties

Moiety	Solid angle (deg) at B	Deviation from planarity (deg) at B	Solid angle (deg) at N	Deviation from pyramidalization (deg) at N
BH_2-NH_2	359.9	0.1	359.0	200.1
BH-$(NH_2)_2$	359.9	0.1	357.7	198.8
B-$(NH_2)_3$	359.5	0.5	307.2	148.3
BH_3-NH_3	219.6	140.4	167.8	8.9
NH-$(BH_2)_2$	359.5	0.5	360.0	201.1
N-$(BH_2)_3$	359.9	0.1	360.0	201.1

4.3.2. Substituent Effect: Deviation from Planarity and Pyramildalisation

Table 4.4 shows the solid angles at B and N and deviations from planarity at B and pyramidalisation at N for the molecules formed by replacing H's attached to B's by electron donating and withdrawing groups.

Table 4.4: The solid angles at B and N and deviations from planarity at B and pyramidalisation at N for the molecules formed by replacing H's attached to B's by electron donating and withdrawing groups

Substituent on B	Solid angle (deg) at B	Deviation from planarity (deg) at B	Solid angle (deg) at N	Deviation from pyramidalization (deg) at N
H	333.0	27.0	214.6	55.7
Cl	352.3	7.7	271.6	112.7
SH	347.8	12.2	241.2	82.3
CH_3	337.7	22.3	231.0	72.1
NH_2	359.9	0.1	247.6	88.7
CN	339.0	21.0	232.7	73.8

The solid angle at B for 1,3-diazadiboretidine (puckered) is 333^0 and for all the substitutions, it is more than that which means that the deviations from planarity at B is lesser than that of the parent molecule. We can also see that for -NH_2 substitution, the solid angle is 359.9^0 making the geometry around B almost planar.

However, no trend can be seen for the solid angles around N. In all the cases, the solid angles at N are somewhere between the planar geometry and pyramidal geometry.

So, it can be concluded that substituting the H's attached to B's is probably not going to help much in our study because we have seen in our calculations that as we do that, deviations from planarity at B decreases (which is not interesting for the problem) instead of increasing.

4.4. Substituting Atoms in the Core Four-Membered Ring

We have seen in the previous section that even after substituting H's attached to B's of our molecule of interest by different electron donating and electron withdrawing groups, the geometry around three coordinated B atom did not deviate much from planarity. So, we opted for a new way. We decided to replace atoms of the core B_2N_2 ring by other atoms to see whether a large deviation from planarity is possible at all or not. Here, either one or both the –NH's have been replaced by other atoms. These will be explained in detail at the results section. Our experimentalist collaborators were interested in having Cl as the substituent at B as it is synthetically more suitable and energetically more favoured. So, for most of the calculations that we have performed in this section; we have used both H and Cl as the substituent at B.

4.4.1. Computational Details

All the geometry optimizations and frequency calculations have been performed at MP2/aug-cc-pVDZ level of theory. The Mulliken populations have been calculated at CISD/aug-cc-pVDZ level. The calculations have been done using Molpro (version 2012.1).[13]

4.4.2. Results and Discussions

The following substitutions have been performed on the core B_2N_2 ring of 1,3-diazadiboretidine (puckered) (and its analogue where H's attached to B's are replaced by Cl): (1) the two –NH's have been replaced by two oxygen atoms, (2) only one –NH has been replaced by an O atom (3) both the –NH's have been replaced by two Sulfur atoms and (4) only one –NH has been replaced by a S atom. All the cases will be discussed one by one.

For case (1), the optimized geometry of cyclo-1,3-$B_2O_2H_2$ (Fig. 4.11) and cyclo-1,3-$B_2O_2Cl_2$ (Fig. 4.12) came out to be planar. The B-O bond length in both the molecules is in the range of single B-O bonds. The B-H bond length is same as the experimental B-H single bond length while the B-Cl bond length is a little less than the average single B-Cl bond (which is 1.75 Å). The HOMO's in both the molecules show that there is no delocalization of electrons in the B_2O_2 ring. Fig. 4.13 shows the HOMO in cyclo-1,3-$B_2O_2H_2$, where we can see that it is the lone pair of electrons localized on the O atoms. Fig. 4.14 shows the HOMO in cyclo-1,3-$B_2O_2Cl_2$, where it is the lone pair of electrons localized on the O atoms and the unpaired electrons localized at Cl atom. There is no delocalisation taking place. The ring puckering is also negligible i.e. there is no puckering involved. Similarly, the deviation from planarity at B atom is also negligible.

Table 4.5: Energy, imaginary Frequency, puckering and deviation from planarity at B for Case (1)

Molecule	**E(MP2/aug-cc-pVDZ) (H)**	**Imaginary Freq.(cm^{-1})**	**Puckering (degree)**	**Solid angle at B (deg.)**	**Deviation from planarity at B (degree)**
Cyclo-1,3-$B_2O_2H_2$	-200.963483	-	0.005	359.9	0.1
Cyclo-1,3-$B_2O_2Cl_2$	-1119.200859	-	0.007	359.7	0.3

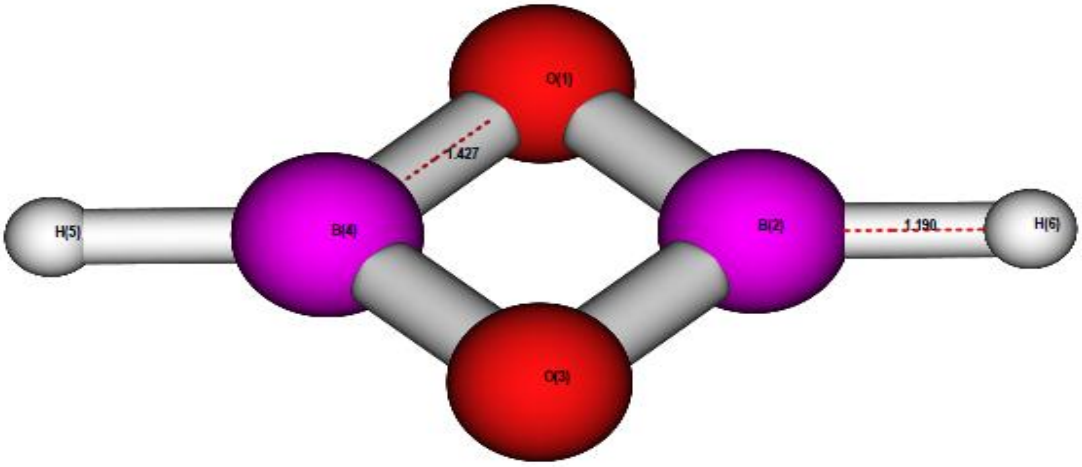

Fig. 4.11: Optimized geometry of cyclo-1,3-$B_2O_2H_2$ at MP2/aug-cc-pVDZ level

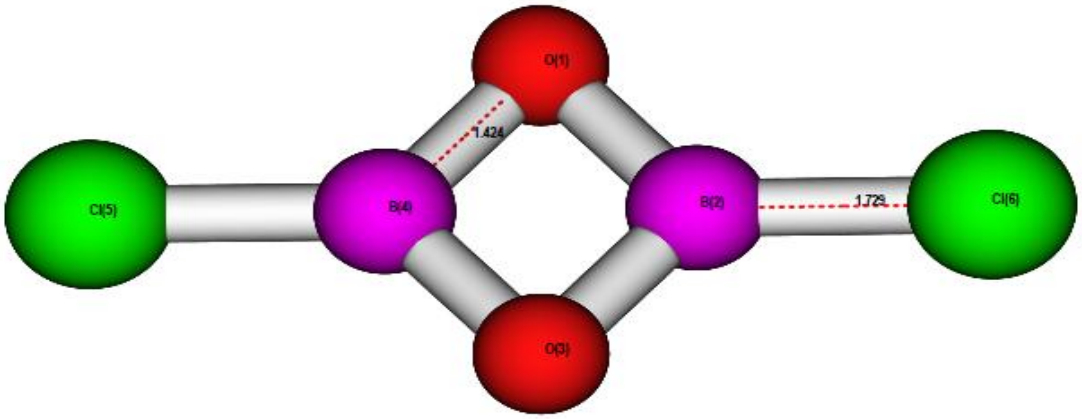

Fig. 4.12: Optimized geometry of cyclo-1,3-$B_2O_2H_2$ at MP2/aug-cc-pVDZ level

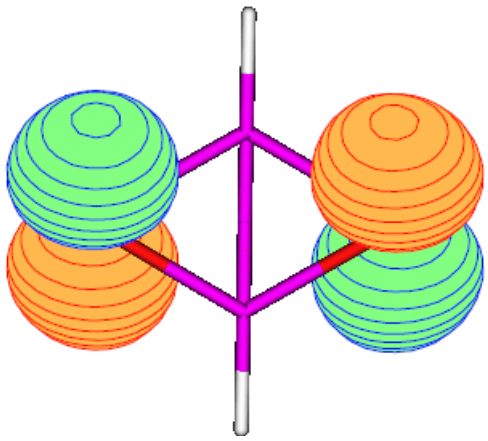

Fig. 4.13: HOMO of cyclo-1,3-$B_2O_2H_2$

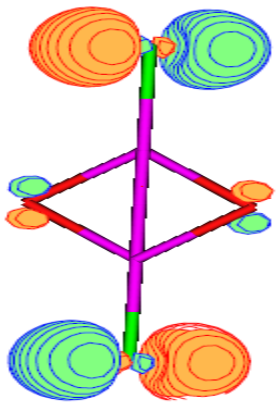

Fig. 4.14: HOMO of cyclo-1,3-$B_2O_2Cl_2$

For case (2), Fig. 4.15 and Fig. 4.16 show the optimized geometry of cyclo-B_2ONH_3 and cyclo-B_2ONHCl_2. The B-O bond length in both the molecules is in the range of single B-O bonds. The B-H, N-H and B-Cl bond lengths are also very close to the experimental values. The HOMO's in both the molecules show that there is no delocalization of electrons in the B_2ON ring. Fig. 4.17 shows the HOMO in cyclo-B_2ONH_3, where we can see that it is the lone pair of electrons localized on the O atom and N atom. Fig. 4.18 shows the HOMO in cyclo-B_2ONHCl_2, where it is the lone pair of electrons localized on the O atoms, N atoms and the unpaired electrons localized at Cl atom. There is no delocalisation taking place. The ring puckering is almost negligible for cyclo-B_2ONHCl_2 while there is an approximate 8^0 ring puckering for cyclo-B_2ONH_3. The deviation from planarity at B atom is also very small.

Table 4.6: Energy, imaginary frequency, puckering and deviation from planarity at B for Case (2)

Molecule	**E(MP2/aug-cc-pVDZ) (H)**	**Imaginary Freq.(cm^{-1})**	**Puckering (degree)**	**Solid angle at B (deg.)**	**Deviation from planarity at B (degree)**
Cyclo-B_2ONH_3	-181.092617	-	8.029	349.2	10.8
Cyclo-B_2ONHCl_2	-1099.334383	-	0.047	359.9	0.1

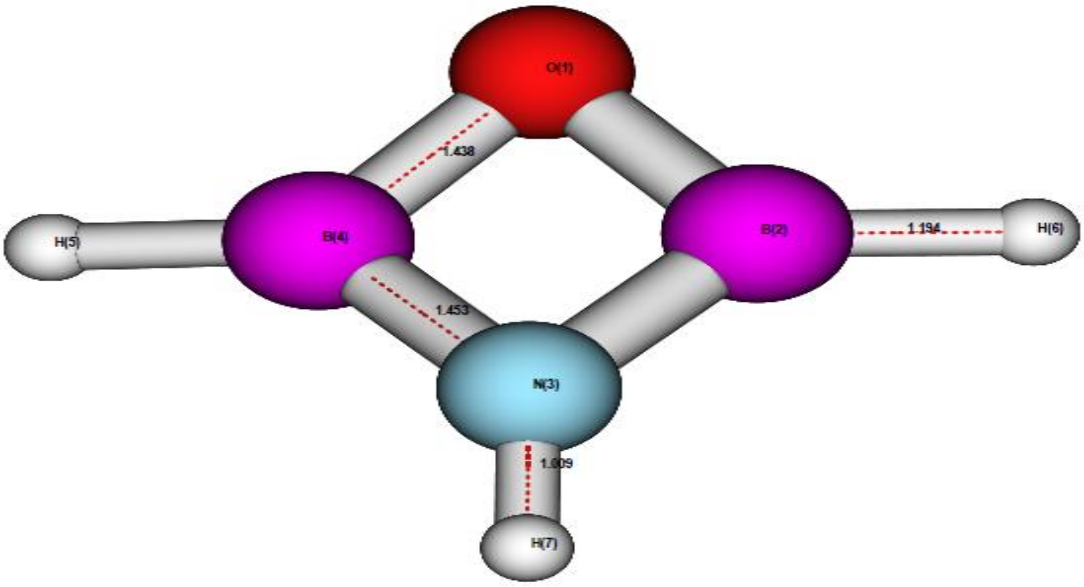

Fig. 4.15: Optimized geometry of cyclo-B_2ONH_3 at MP2/aug-cc-pVDZ level

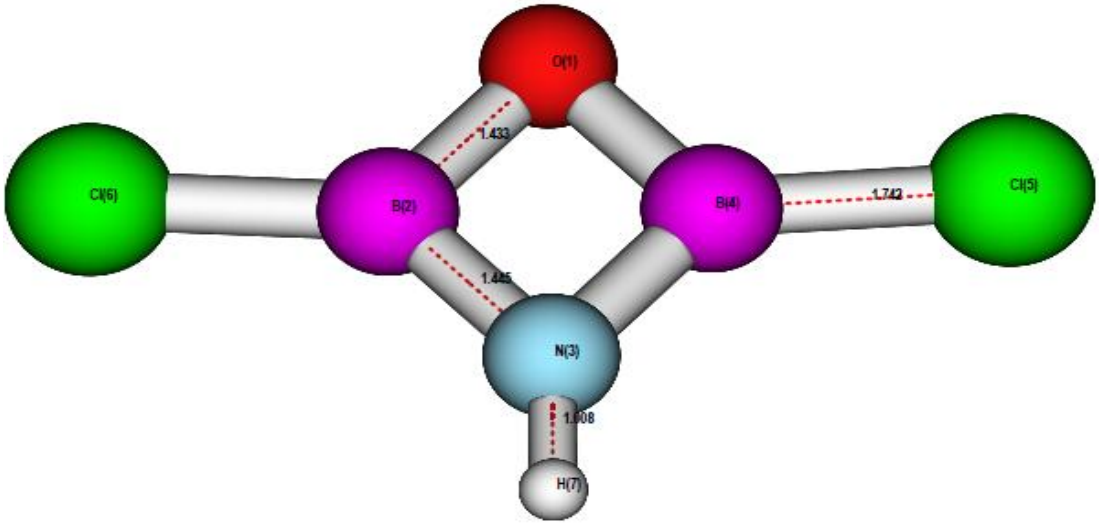

Fig. 4.16: Optimized geometry of cyclo-B_2ONHCl_2 at MP2/aug-cc-pVDZ level

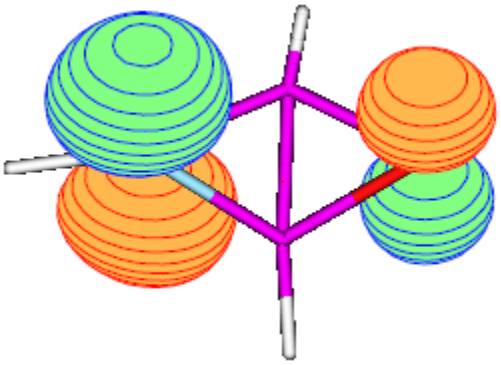

Fig. 4.17: HOMO of cyclo-B_2ONH_3

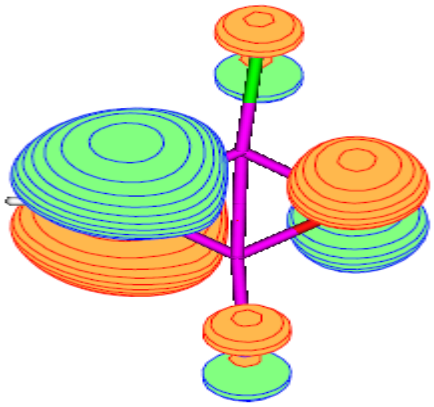

Fig. 4.18: HOMO of cyclo-B_2ONHCl_2

For case (3), Fig. 4.19 and Fig. 4.20 show the optimized geometry of cyclo-1,3-$B_2S_2H_2$ and cyclo-1,3-$B_2S_2Cl_2$. The B-S bond length in both the molecules is in the range of single B-S bonds. The B-H and B-Cl bond lengths are also very close to the experimental values. The HOMO's in both the molecules show that there is no delocalization of electrons in the B_2S_2 ring. Fig. 4.21 shows the HOMO in cyclo-1,3-$B_2S_2H_2$ and Fig. 4.22 shows the HOMO in cyclo-1,3-$B_2S_2Cl_2$. In both the cases, we can see that it is the lone pair of electrons localized on the S atoms which means that there is no delocalisation taking place. Although there is quite enough puckering in cyclo-1,3-$B_2S_2H_2$, the puckering in cyclo-1,3-$B_2S_2Cl_2$ is almost negligible. The deviation from planarity at B is negligible for cyclo-1,3-$B_2S_2Cl_2$. However, the deviation from planarity at B for cyclo-1,3-$B_2S_2H_2$ is 30.8^0. But, as the puckering is also little high for the system, that also contributes to the deviation from planarity.

Table 4.7: Energy, imaginary frequency, puckering and deviation from planarity at B for Case (3)

Molecule	**E(MP2/aug-cc-pVDZ) (H)**	**Imaginary Freq.(cm^{-1})**	**Puckering (degree)**	**Solid angle at B (deg.)**	**Deviation from planarity at B (degree)**
Cyclo-1,3-$B_2S_2H_2$	-846.123076	-	19.005	329.2	30.8
Cyclo-1,3-$B_2S_2Cl_2$	-1764.364676	-	0.013	359.97	0.03

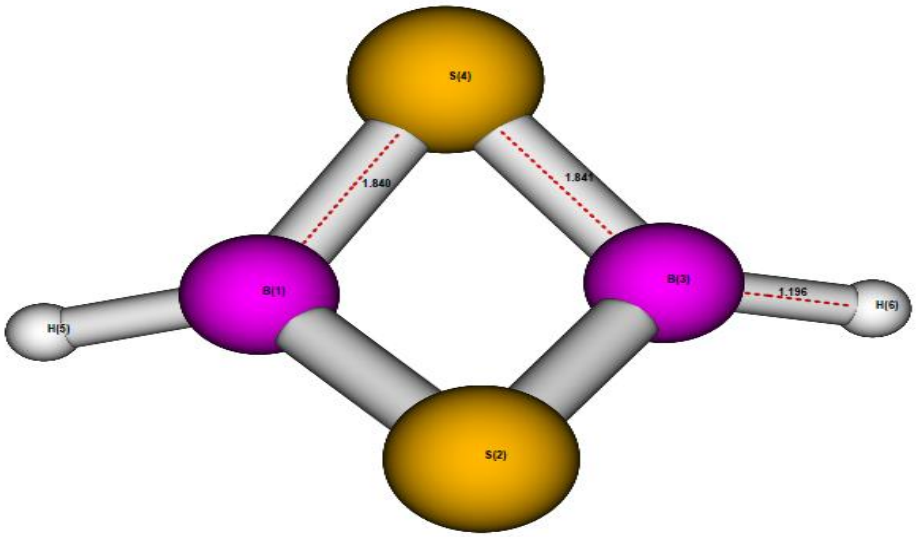

Fig. 4.19: Optimized geometry of cyclo-1,3-$B_2S_2H_2$ at MP2/aug-cc-pVDZ level

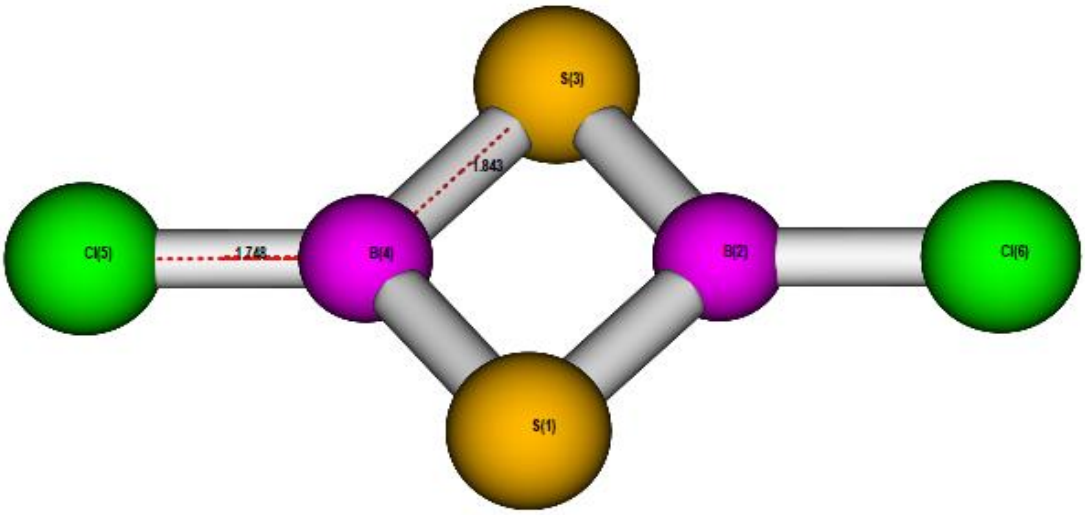

Fig. 4.20: Optimized geometry of cyclo-1,3-$B_2S_2Cl_2$ at MP2/aug-cc-pVDZ level

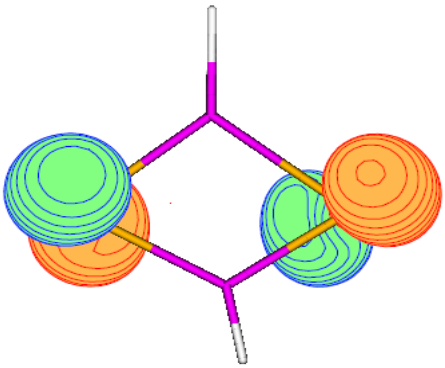

Fig. 4.21: HOMO of cyclo-1,3-$B_2S_2H_2$

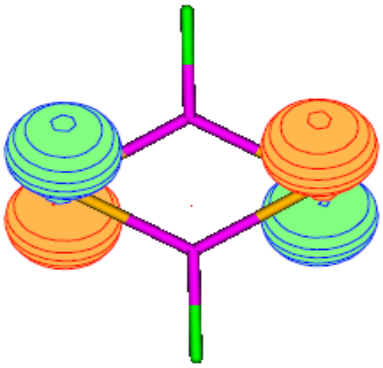

Fig. 4.22: HOMO of cyclo-1,3-$B_2S_2Cl_2$

For case (4), Fig. 4.23 and Fig. 4.24 show the optimized geometry of cyclo-B_2SNH_3 and cyclo-B_2SNHCl_2. The B-S bond length in both the molecules is in the range of single B-S bonds. The B-H, N-H and B-Cl bond lengths are also very close to the experimental values. The HOMO's in both the molecules show that there is no delocalization of electrons in the B_2SN ring. Fig. 4.25 shows the HOMO in cyclo-B_2SNH_3, where we can see that it is the lone pair of electrons localized on the S atom and N atom. Fig. 4.26 shows the HOMO in cyclo-B_2SNHCl_2, where also the situation is same i.e. there is no delocalisation taking place. Although there is quite enough puckering in cyclo-B_2SNH_3, the puckering in cyclo-B_2SNHCl_2 is very small. The deviation from planarity at B for cyclo-B_2SNHCl_2 is negligible while that for cyclo-B_2SNH_3 is 23.6^0. But, still the deviation is not sufficient enough.

Table 4.8: Energy, imaginary frequency, puckering and deviation from planarity at B for Case (4)

Molecule	**E(MP2/aug-cc-pVDZ) (H)**	**Imaginary Freq.(cm^{-1})**	**Puckering (degree)**	**Solid angle at B (deg.)**	**Deviation from planarity at B (degree)**
Cyclo-B_2SNH_3	-503.679083	-	13.042-15.521	336.4	23.6
Cyclo-B_2SNHCl_2	-1421.922159	-	0.159-0.191	359.8	0.2

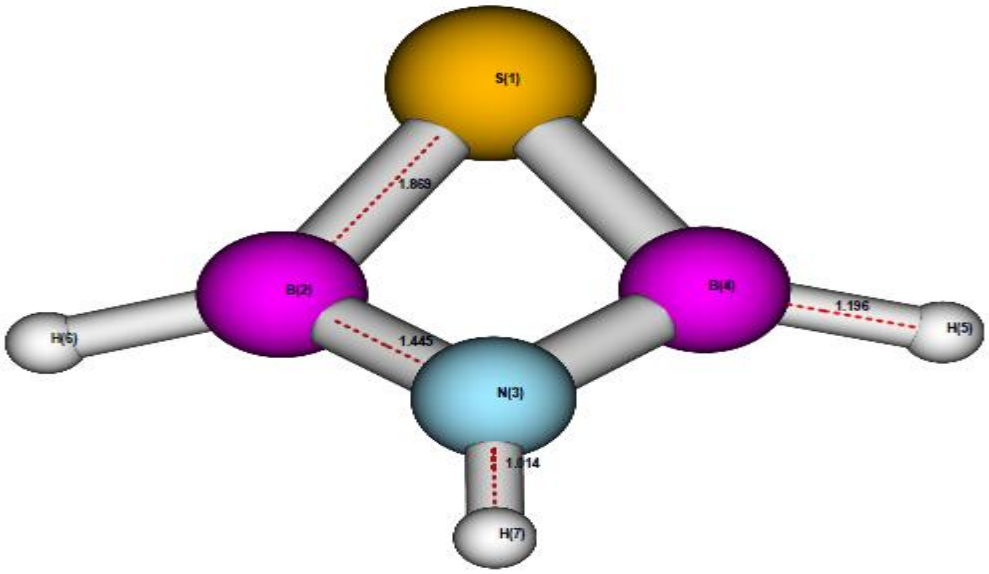

Fig. 4.23: Optimized geometry of cyclo-B_2SNH_3 at MP2/aug-cc-pVDZ level

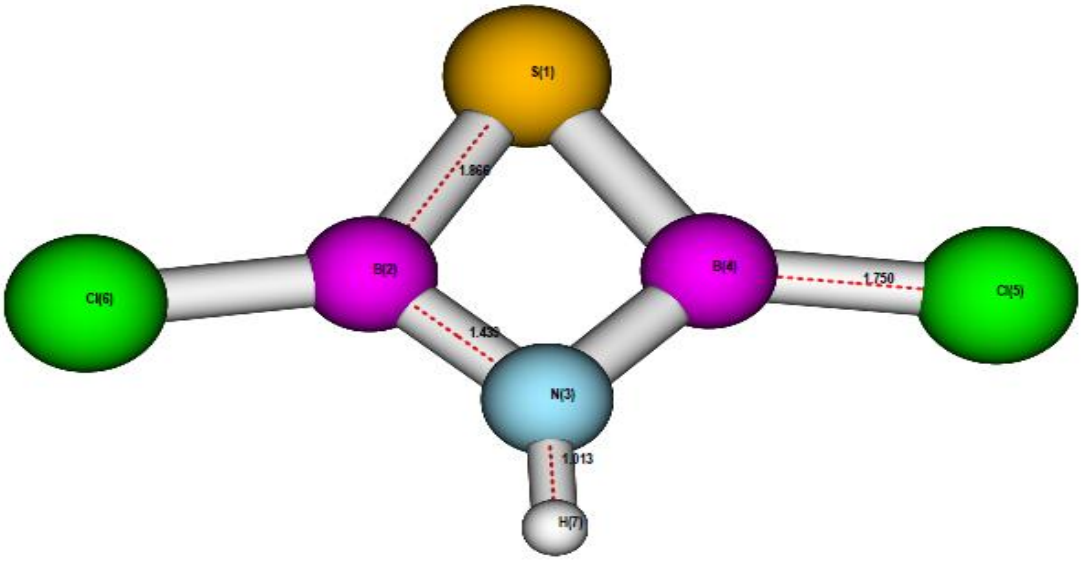

Fig. 4.24: Optimized geometry of cyclo-B_2SNHCl_2 at MP2/aug-cc-pVDZ level

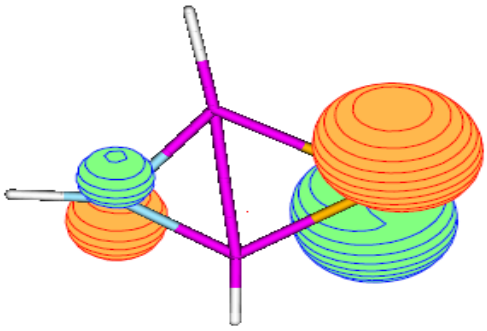

Fig. 4.25: HOMO of cyclo-B_2SNH_3

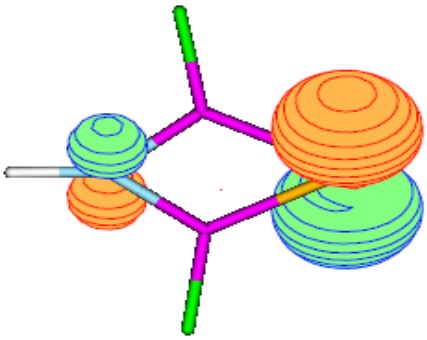

Fig. 4.26: HOMO of cyclo-B_2SNHCl_2

Table 4.9 shows the charge on B atoms for each of the cases considered in this section. The charge on B for each of the molecules came out to be positive as expected. However, it can be easily observed that in each of the case, when H's attached to B's were replaced by Cl's, the positive charge on B atom increased slightly. It is the electron withdrawing nature of Cl that increased the positive charge on B in those molecules.

Table 4.9: Charge on B atoms for each of the above mentioned cases

Case	Molecule	Charge on B
1	Cyclo-1,3- $B_2O_2H_2$	0.303
	Cyclo-1,3- $B_2O_2Cl_2$	0.327
2	Cyclo- B_2ONH_3	0.236
	Cyclo-B_2ONHCl_2	0.273
3	Cyclo-1,3-$B_2S_2H_2$	0.112
	Cyclo-1,3-$B_2S_2Cl_2$	0.183
4	Cyclo- B_2SNH_3	0.146
	Cyclo-B_2SNHCl_2	0.196

All the substitutions at B and substitutions in the core ring were unable to distort the geometry around B much from planarity. Another aspect that we have noted is that Cl substitution at B actually makes the molecule more stable than all other substitutions. So, from experimentalist point of view, Cl substituted ones will be relatively easier to isolate than others if it is possible at all to isolate them. However, the deviation from planarity at B is highest for H's attached to B's only. So, we decided to concentrate on boron's electron affinity and performed multireference calculations of anions and dianions related to that which is reported in details in chapter 5.

4.5. Different System Altogether

We also considered changing the whole system. The core B_2N_2 ring has been replaced with P_2N_2 ring. Our interest was in systems like [Cyclo-1,3-$P_2N_2R_2$]$^{2+}$. We have performed calculations with R = -H, -CH_3. After we found the optimized geometries of this type of rings, we went on to calculate the optimized geometries of these rings where we attached Cl at P atom and made 3-coordinated phosphorus. It is known that P forms a pyramidal structure in PCl_3. Our interest was to see if the same thing happens in these rings too. All the calculations have been done at MP2/aug-cc-pVDZ level for these systems in Molpro (version 2012.1).[13]

Fig. 4.27 and Fig.4.28 shows the optimized geometries of cyclo-1,3-$P_2N_2Cl_2H_2$ and cyclo-1,3-$P_2N_2Cl_2(CH_3)_2$. For, both the optimized geometries, P-N and P-Cl are both single bonds. The N-H bond length also suggests a single bond in cyclo-1,3-$P_2N_2Cl_2(CH_3)_2$. Even the C-N bond (1.45 Å) in cyclo-1,3-$P_2N_2Cl_2(CH_3)_2$ is forming a single bond. The HOMOs of both the molecules show that the electrons are localized on P, N and Cl atoms. Both the rings are quite puckered in case of the neutral molecules. There is a large deviation from planarity at P for both the neutral molecules (which is because of the localised electrons on P) that we have not seen earlier in our study in B based rings. The geometry around P is more inclined towards pyramidal and the P-Cl bonds are cis to each other and bent a huge amount with respect to the core P_2N_2 ring.

Table 4.10: Energy, imaginary frequency, puckering and deviation from planarity at P for cyclo-1,3-$P_2N_2Cl_2H_2$ and cyclo-1,3-$P_2N_2Cl_2(CH_3)_2$

Molecule	**E(MP2/aug-cc-pVDZ) (H)**	**Imaginary Freq.(cm^{-1})**	**Puckering (degree)**	**Solid angle at B (deg.)**	**Deviation from planarity at B (degree)**
Cyclo-1,3-$P_2N_2Cl_2H_2$	-1711.521068	-	12.208	255.0	105.0
Cyclo-1,3-$P_2N_2Cl_2(CH_3)_2$	-1789.886499	-	7.181	252.9	107.1

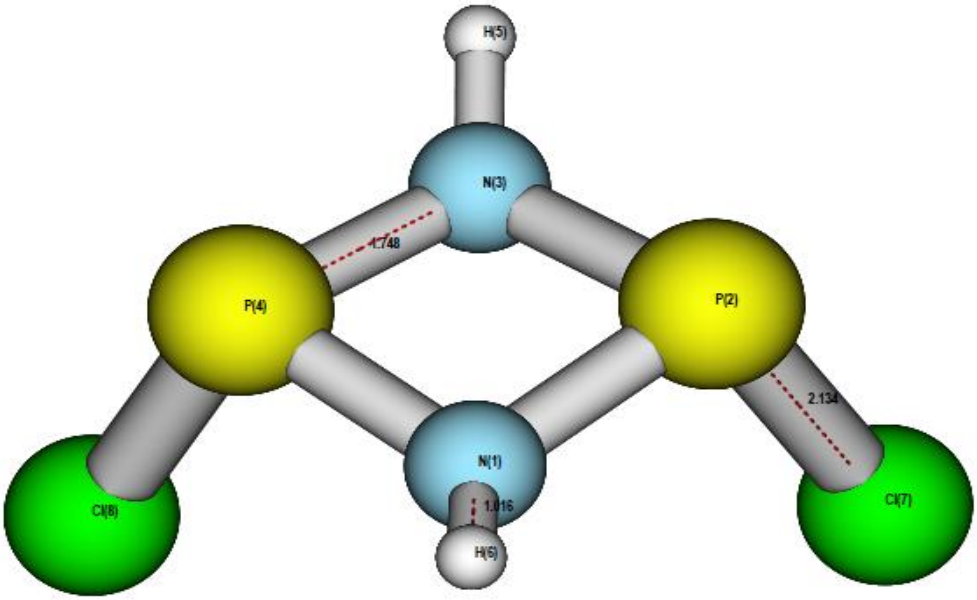

Fig. 4.27: Optimized geometry of cyclo-1,3-$P_2N_2Cl_2H_2$ at MP2/aug-cc-pVDZ level

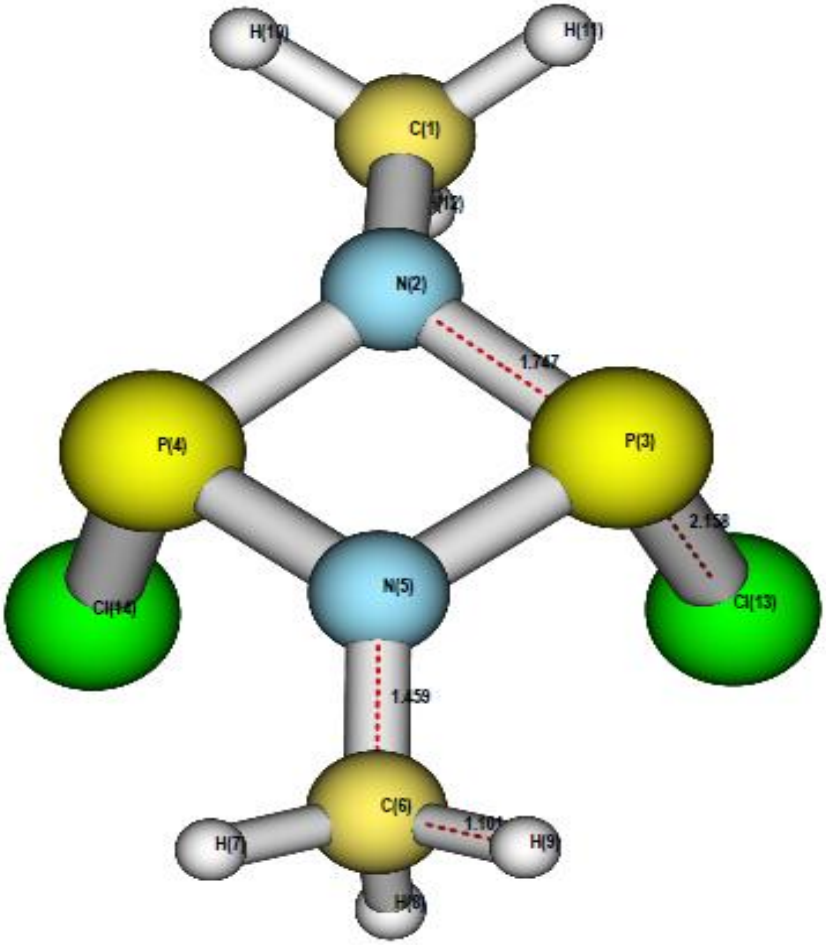

Fig. 4.28: Optimized geometry of cyclo-1,3-$P_2N_2Cl_2(CH_3)_2$ at MP2/aug-cc-pVDZ level

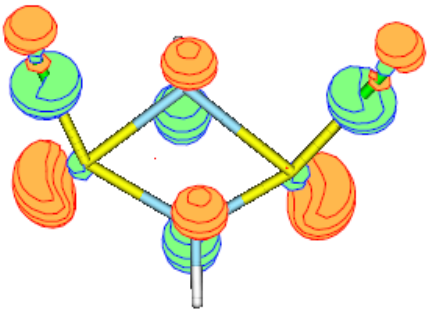

Fig. 4.29: HOMO of cyclo-1,3-$P_2N_2Cl_2H_2$

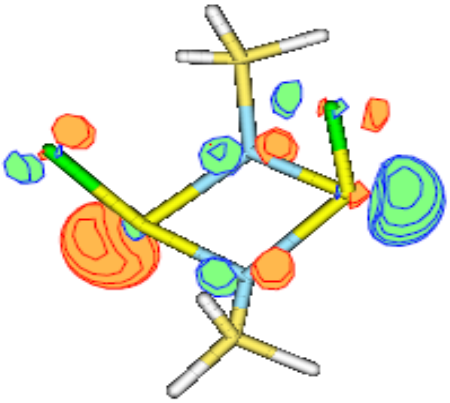

Fig. 4.30: HOMO of cyclo-1,3-$P_2N_2Cl_2(CH_3)_2$

4.6. Conclusion and Future Outlook

We have seen the effect of substituting different electron donating and electron withdrawing groups at B of our parent molecule and also substituting different atoms in the core B_2N_2 ring. However, it was not possible, in boron based rings, to achieve a large deviation from planarity around B atom which may facilitate the formation of macro cycle. There is still a way to look at the problem which was not investigated properly because of the time constraint. We can replace the H's attached to N atoms in 1,3-diazadiboretidine (puckered) by sterically hindered ligands [for example, methyl (-Me), tertiary butyl (-tBu), phenyl (-Ph) etc] and perform calculations to see if the steric bulk of these ligands can deviate the geometry around B by a large amount.

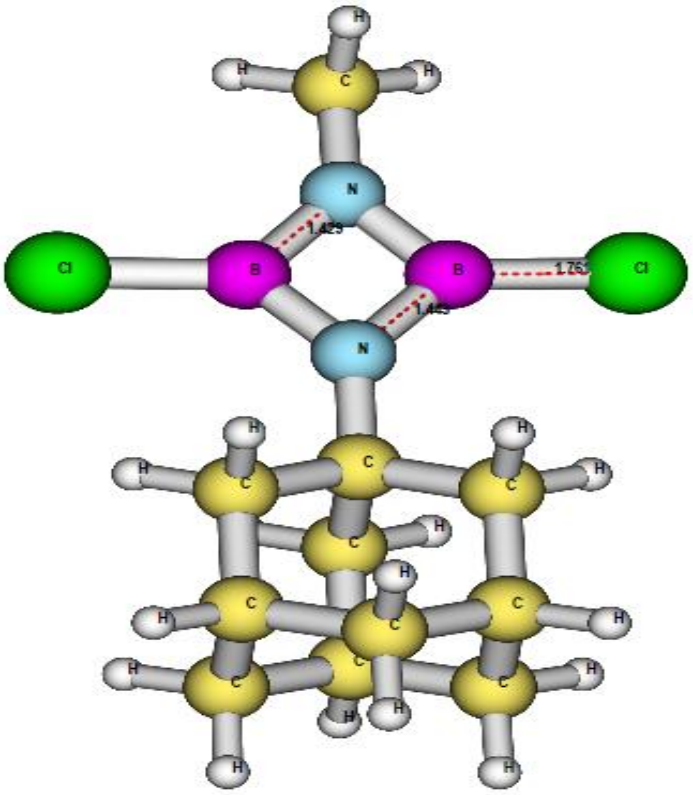

Fig. 4.31: Optimized geometry a hypothetical molecule where one H attached to N is replaced by an –Ad (adamantane) group and the other by methyl group at HF/6-31G* level

Fig. 4.31 shows the optimized geometry a hypothetical molecule of this type where one H attached to N is replaced by an –Ad (adamantane) group and the other by methyl group. The optimization has been performed at HF/6-31G* level of theory as MP2 level would have been a lot costly from computational point. The molecule has a ring puckering in the range 3.083^0-3.106^0. But, the deviation from planarity at B is small and also the presence of an imaginary frequency suggests that it is actually a local maximum.

However, this view has not been investigated properly as the systems of interest are large and the calculations in MP2/aug-cc-pVDZ level of theory will be computationally a lot costly. Although a few of these systems have been investigated using the aforementioned level of theory where H's attached to N's have been replaced by methyl groups, the deviations from planarity at B were found to be small and similar to the values found in section 4.3.2. So, this is something that needs to be looked at properly in future and probably the best way to investigate this type of systems is to use DFT.

Chapter 5

Study on Monoanions and Dianions

5.1. Boron: Its Electron Deficiency and Electron Affinity

Boron is electron deficient in terms of octet. So, it should have a high electron affinity. But, contrary to that, B has a very low electron affinity value with respect to other electron deficient atoms of the same period. As can be seen from the Table 5.1, B has lesser electron affinity values than Li, C, O and F in the second period.

Table 5.1: Electron affinity values of 2nd period (KJ/mol)

Li	Be	B	C	N	O	F	Ne
59.8	<0	27.0	122.3	<0	141.1	328.0	<0

So, not only B is electron deficient, it also is such an atom that does not want to accept electrons. This is a very important aspect for our study. Our main aim was to find a way to bend or pyramidalize the 3-coordinated geometry around B, which we have tried with different electron withdrawing and electron donating substituents. Substitutions were also performed on the core ring to do the same. As the results were not promising, a different approach has been tried.

5.2. Study on the Monoanion of BH_3

It is known that borane (BH_3) has a planar geometry and the B atom is 3-coordinated. Our interest was to see the effect of introducing a negative charge i.e. an electron in the BH_3 system. We wanted to see whether BH_3 has the capability of accepting an electron or not and if it can, whether the structure becomes pyramidal or prefers to stay planar.

5.2.1. Computational Details

The initial geometry has been generated using dummy atom as shown in Fig. 5.1. The angle θ shown in the Fig. 5.1 was the variable that was varied and all other variables have been optimized. This constrained optimization has been performed at MRSDCI/aug-cc-pVDZ level of theory in Molpro (2012.1).[13] In this calculation, the reference wave function was CAS (10o,8e).

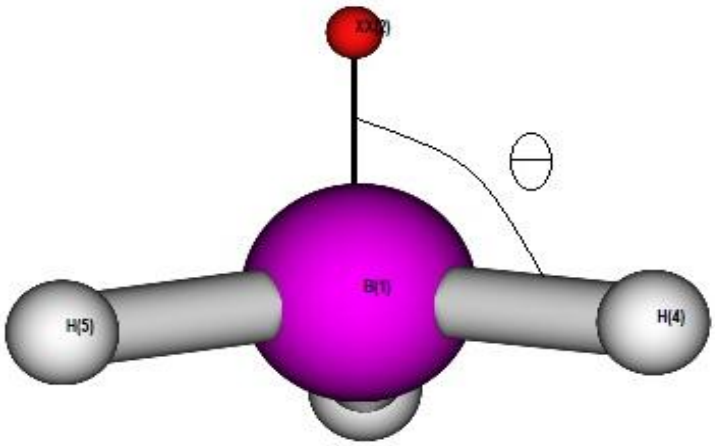

Fig. 5.1: Definition of angle θ in the initial guess geometry of BH3-

5.2.2. Results and Discussion

The energy of the BH_3 monoanion have been plotted at different values of θ to generate a PES. Fig. 5.2 shows the PES scans of S_0 and S_1 state of BH_3^-. The minimum energy was scaled to zero and all other energy values were plotted with respect to that. S_0 and S_1 were the two lowest lying states of BH_3^-. Although, both the PES's were flat, the minimum was achieved at 90^0 for both the states which suggest that even the single anion of BH_3 prefers a planar geometry. The extra negative charge is unable to distort or pyramidalize it.

We have also been interested in electron affinity of BH_3. Electron Affinity of BH_3 can be defined as the difference between the total electronic energy of BH_3 and that of BH_3^-. We looked at the literature and found out that there had been some important work in this aspect. Gutsev et al. found out that at the CCSD(T) level of theory, the difference in the total electronic energy of BH_3 and that of BH_3^- is -0.05 eV. However, when they corrected their calculations for the zero-point energies

(ZPE) of nuclear motions, the adiabatic electron affinity (EA-ad) of BH_3 came out to

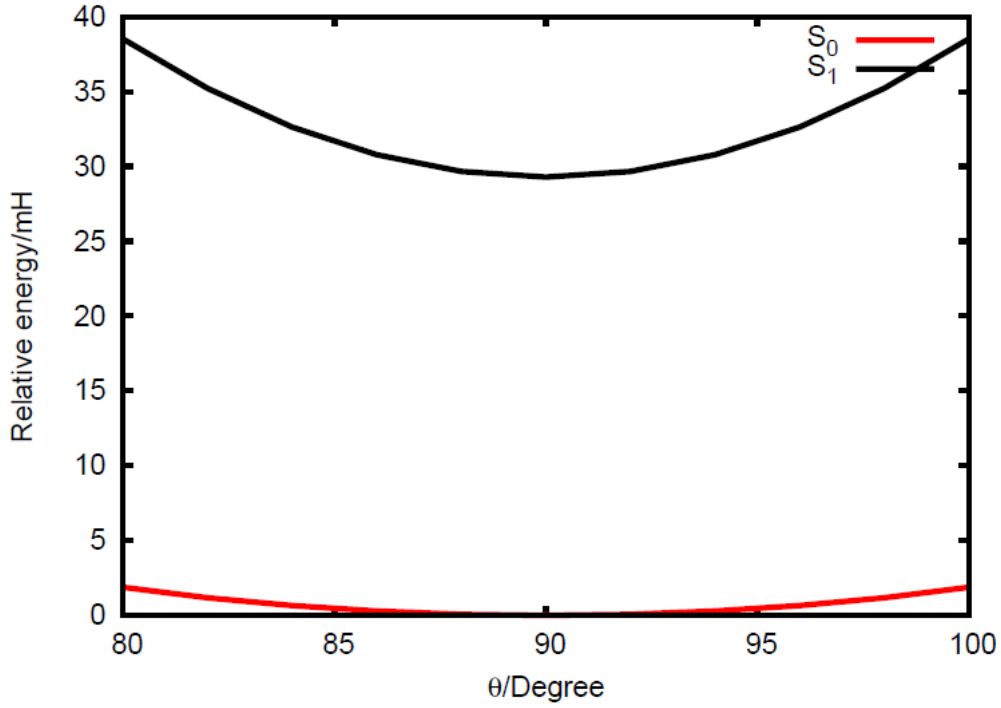

Fig. 5.2: PES scans of S_0 and S_1 state of BH_3^-

be 0.01 eV, which was in nice agreement with the experimental value 0.038(+/-) 0.015.[16] Grant et al. also calculated electron affinities of different molecules at 0 K at the CCSD(T)/CBS level of theory.[17] In one case, they studied electron affinity of BH_3 and along with that, they substituted Cl's in place of H's of BH_3 one by one and calculated their electron affinities too. The calculations showed that as Cl's were substituted one after another, the electron affinities increased, BCl_3 having the highest EA among them. Table 5.2 shows the calculated electron affinites at 0 K at CCSD(T)/CBS level.

Table 5.2: The calculated electron affinites at 0 K at CCSD(T)/CBS level[17]

Molecule	CCSD(T) (eV)	CCSD(T) (Kcal/mol)	Experimental (eV)
BH_3	0.031	0.8	0.038 ± 0.015
H_2BCl	0.05	1.4	-
$HBCl_2$	0.22	5.8	-
BCl_3	0.49	12.7	0.33 ± 0.20

So, from these studies, it was understood that not only boron, even BH_3 molecule does not like to accept a single electron and even if it accepts, the single anion prefers to be in planar geometry.

5.3. Future Outlook

5.3.1. Study on the Dianion of cyclo-1,3-$B_2N_2H_4$

We have also been interested to see if placing two negative charges on 1,3-diazadiboretidine (puckered) can distort the geometry around B atoms. In case of dianions, computational studies are a lot harder than the neutral molecules and cations and very careful multireference calculations are needed. We took the optimized geometry of the above mentioned molecule at MP2/aug-cc-pVDZ level, added two negative charges and performed MRSDCI single point energy calculation. The reference wavefunction was CAS (6o,4e). On top of that single point MRSDCI single point calculation has been done. In Fig. 4.3, we have shown the energy difference between the four lowest lying states S_0, S_1, S_2 and S_3 in both MCSCF and MRSDCI method. The two lowest lying states have been optimized at MRSDCI/aug-cc-pVDZ level. The calculations have been performed in Molpro (2012.1)[13]. The energy difference between S_0 and S_1 states (Fig. 5.4) were found to be 13.016 Kcal/mol.

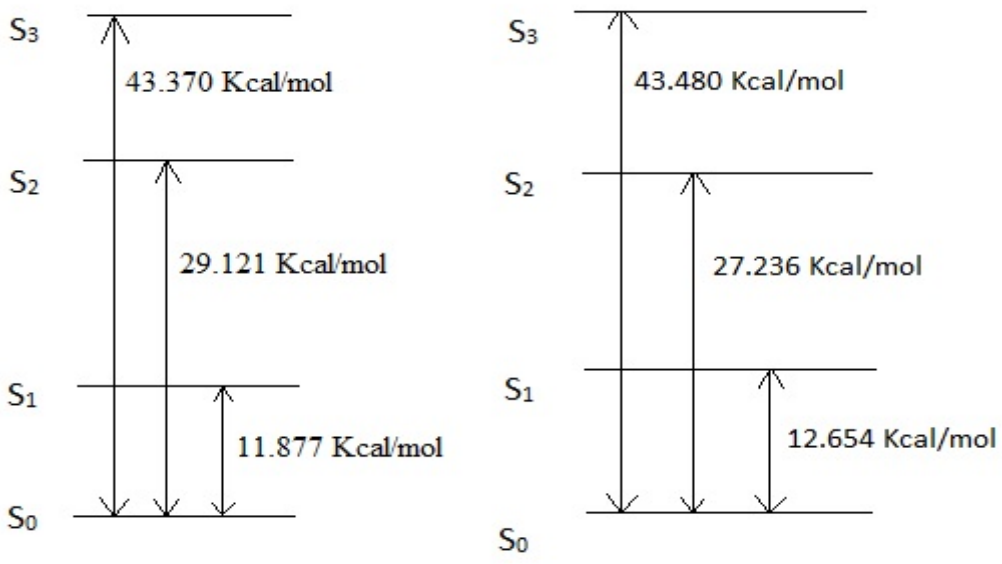

Fig. 5.3: The energy difference between the four lowest lying states S_0, S_1, S_2 and S_3 in both MCSCF (left) and MRSDCI (right) method for the dianion of 1,3-diazadiboretidine (puckered)

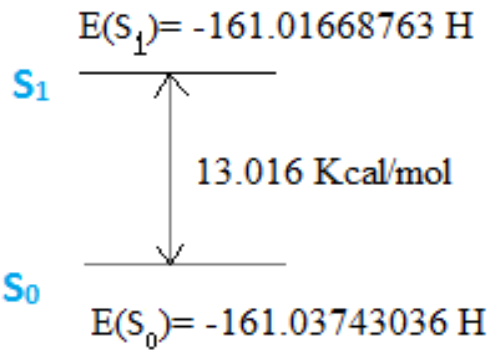

Fig. 5.4: The energy difference between the lowest lying states S_0 and S_1 for 1,3-diazadiboretidine (puckered)

Because of the two negative charges, it is important investigate whether the dianion has a diradical character or not. Diradicals are molecules where two electrons occupy two near degenerate orbitals.[18] The natural occupation numbers of HOMO and LUMO of a molecule determine the extent of diradical character of a molecule. In a purely closed shell system, the occupation numbers of HOMO and LUMO are 2 and 0 respectively. When the occupation numbers of HOMO and LUMO are both equal and 1, then, the system is a pure diradical.[19, 20] In our case, for the dianion, the occupation number of HOMO and LUMO came out to be 1.208 and 0.792 respectively for the lowest lying S_0 state. This suggests that there may be a certain amount of diradical charater associated with our system. The deviation from planarity at B is also small for the S_0 state of the dianion just like the neutral molecule. However, this calculation was just performed for an active space and we cannot trust these results yet. A few more calculations need to be performed by changing the active space and then we can confirm if it has a diradical character or not.

5.3.2. Study on the Monoanion and Dianion of BCl_3

We have also been interested to study the monoanion and dianion of BCl_3 as reactions are easier to perform with Cl. BCl_3 has a planar geometry and it was in our interest to see if it can deviate from its planar geometry when we introduce one or two electrons in the system. We defined θ the same way as in Fig. 5.1. We have optimized the neutral BCl_3, anion and dianion of BCl_3 in Molpro (version 2012.1)[13]. Table 5.3 shows the data needed to analyze them.

Table 5.3: Level of theory, energy and variables for BCl_3, BCl_3^- and BCl_3^{2-}

System	Level of Theory	Energy (H)	B-Cl bond (Å)	θ (degree)
BCl_3	CCSD/aug-cc-pVDZ	-1403.883414	1.760	90.0
BCl_3^-	RCCSD/aug-cc-pVDZ	-1403.901335	1.880	107.0
BCl_3^{2-}	CISD/aug-cc-pVDZ	-1403.647010	2.197	118.5
BCl_3^{2-}	CCSD/aug-cc-pVDZ	-1403.749968	2.193	118.5
BCl_3^{2-}	RS2C/aug-cc-pVDZ	-1403.719348	2.197	118.3
BCl_3^{2-}	MRSDCI/aug-cc-pVDZ	-1403.657255	1.932	111.9

BCl_3, as we know it, is planar as $\theta=90.0^0$ (deviation from planarity in terms of solid angle=0.1^0) and has a B-Cl bond which is a normal single bond. When we added an electron in BCl_3 and minimized the energy, we have found that it accepted the electron and got lowered in energy. It also got deviated from planarity as $\theta=107.0^0$ (deviation from planarity in terms of solid angle at B=161.4^0). However, the bond length B-Cl got distorted to a larger 1.88 Å. When we placed two electrons in the system and did the calculations, then the energy increased. The geometry of the dianion gets more distorted or bend as θ increases, and along with that the B-Cl bond length also increases. The added electrons in the dianion goes to the vacant p orbital of B (becomes closed shell) and thus, make it pyramidal. This is really an interesting point for our study. We are able to show that it is possible to deviate the geometry around B in BCl_3 when we add one or two electrons in it. Now, in the gascious state, the monoanion is most stable and so, the dianion will autoionize back to monoanion.

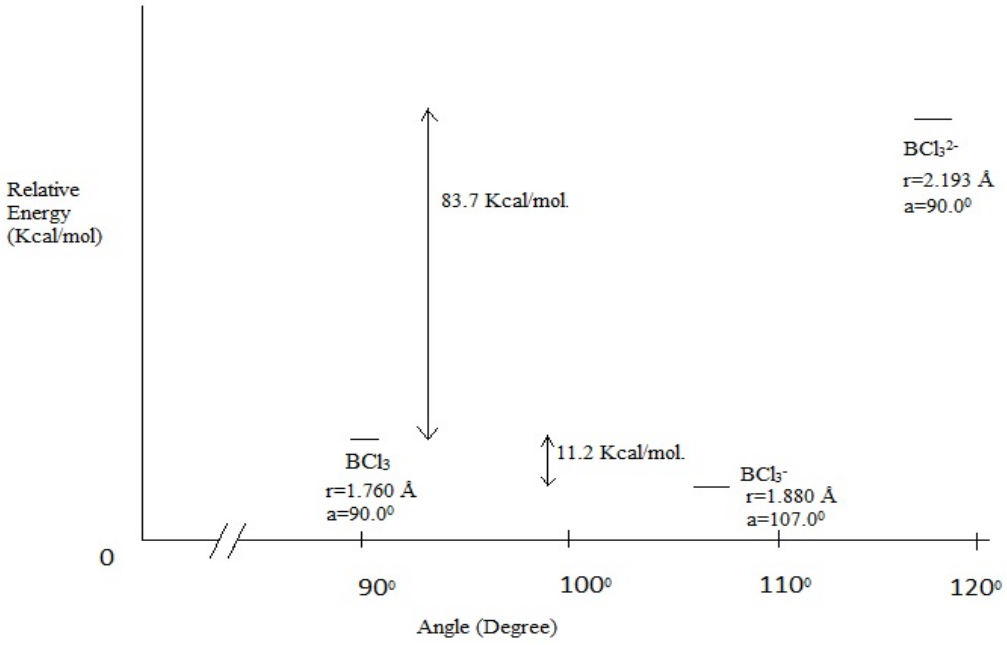

Fig. 5.5: First and second adiabatic electron affinities for BCl_3

However, things may change a lot in case of solution phase. In solution phase, if we can do some substitutions which will force two electrons to the vacant p orbital of B, we might be able to get a stable molecule with highly distorted geometry around B. In all of our study done in Chapter 4 for B based rings, we were unable to find that kind of systems. But, this study shows that we probably need to investigate more on that. Fig. 5.5 shows the first and second adiabatic electron affinities for BCl_3.

Even, more studies need to be done to understand what actually happens to the variables in the dianion of BCl_3. The two single-reference methods and one multireference (RS2C) method optimization converges to the same point for the dianion which has approximately 237.4^0 deviation from planarity (in terms of solid angle). However, in the MRSDCI method optimization, the deviation decreases by some amount and becomes 197.0^0 as θ decreases and the B-Cl bond length also decreases. More calculations need to be done in future to understand the optimized geometry of the dianion.

Chapter 6

Conclusion

In our study, we have verified that puckered conformation of 1,3-diazadiboretidine is the most stable among all the three conformations. We have also performed a detailed study on the above mentioned molecule and confirmed that the optimized structure that we have found is the global minimum of the molecule and it has a C_{2v} symmetry. We replaced the H's attached to B's on the above mentioned molecule by different electron withdrawing and electron donating groups and also replaced the atoms (other than B's) inside the core ring in an effort to see if it is possible to deviate the planar geometry surrounding B atom by a large amount. We were unable to get that in any of the boron based cases until we used a phosphorus based core ring. The B-N bond lengths, Mulliken populations of B (N also in some cases), deviation from planarity at B (and deviation from pyramidalisation at N at some cases) have been analysed thoroughly. We have also found out that even after adding a negative charge to borane, it still prefers to stay planar. However, when we studied the monoanion and dianion of BCl_3, we found that they prefer non-planar geometries and the deviation from planarity is also huge. This is very promising for our study. Our conclusion is that if we can find proper substituents in solution phase, which can force two electrons in the vacant orbitals of B, we might be able to find stable geometries where the two Cl's attached to B's are cis to one another and bent by a large amount which will probably facilitate formation of macro cycles. We still have not tried the problem properly by replacing H's attached to N's of the 1,3-diazadiboretidine (puckered) by sterically hindered groups. This approach needs be investigated carefully before we can confirm anything.

Bibliography

(1) Gaussian 09, Revision D.01, Frisch, M. J.; Trucks, G. W.; Schlegel, H. B.; Scuseria, G. E.; Robb, M. A.; Cheeseman, J. R.; Scalmani, G.; Barone, V.; Mennucci, B.; Petersson, G. A.; Nakatsuji, H.; Caricato, M.; Li, X.; Hratchian, H. P.; Izmaylov, A. F.; Bloino, J.; Zheng, G.; Sonnenberg, J. L.; Hada, M.; Ehara, M.; Toyota, K.; Fukuda, R.; Hasegawa, J.; Ishida, M.; Nakajima, T.; Honda, Y.; Kitao, Nakai, O. H.; Vreven, T.; Montgomery, Jr., J. A.; Peralta, J. E.; Ogliaro, F.; Bearpark, M.; Heyd, J. J.; Brothers, E.; Kudin, K. N.; Staroverov, V. N.; Kobayashi, R.; Normand, J.; Raghavachari, K.; Rendell, A.; Burant, J. C.; Iyengar, S. S.; Tomasi, J.; Cossi, M.; Rega, N.; Millam, J. M.; Klene, M.; Knox, J. E.; Cross, J. B.; Bakken, V.; Adamo, C.; Jaramillo, J.; Gomperts, R.; Stratmann, R. E.; Yazyev, O.; Austin, A. J.; Cammi, R.; Pomelli, C.; Ochterski, J. W.; Martin, R. L.; Morokuma, K.; Zakrzewski, V. G.; Voth, G. A.; Salvador, P.; Dannenberg, J. J.; Dapprich, S.; Daniels, A. D.; Farkas, Ö.; Foresman, J. B.; Ortiz, J. V.; Cioslowski, J.; Fox, D. J.; Gaussian, Inc., Wallingford CT, **2009**

(2) Baceiredo, A.; Bertrand, G.; Majoral, J. P.; Sicard, G.;Juad, J.; Galy, J. *J. Am. Chem. Soc.* **1984**, *106*, 6088

(3) Baird, N. C. *Inorg. Chem.* **1973**, *12*, 473

(4) Baird, N. C.; Whitehead, M. A. *Can. J. Chem.* **1967**, *45*, 2059

(5) Armstrong, D. R.; Clark, D. T. *Theor. Chim. Acta*. **1972**, *24*, 307

(6) Kiran, B.; Phukan, A. K.; Jemmis, E. D. *Inorg. Chem.* **2001**, *40*, 3615

(7) Rehaman, A.; Datta, A.; Mallajosyula, S. S.; Pati, S. K. *J. Chem. Theory Comput.* **2006**, *2*, 30

(8) Tricamo, A. J.; Knaus, K. J.; Ball, D. W. *J. Mol. Struc. Theochem.* **2007**, *807*, 67

(9) Quantum Chemistry, Ira N. Levine, PHI Learning Private Limited, Sixth Edition

(10) Modern Quantum Chemistry, Szabo and Ostlund, Dover Publications Inc., New

York, First Edition

(11) Introduction to Computational Chemistry, Frank Jensen, John Wiley & Sons Ltd., Second Edition

(12) Raghavachari, K.; Anderson, J. B. *J. Phys. Chem.* **1996**, *100***,** 12960

(13) MOLPRO, version 2012.1, a package of ab initio programs, Werner, H.-J.; Knowles, P. J.; Knizia, G.; Manby, F. R.; Schütz, M.; Celani, P.; Korona, T.; Lindh, R.; Mitrushenkov, A.; Rauhut, G.; Shamasundar, K. R.; Adler, T. B.; Amos, R. D.; Bernhardsson, A.; Berning, A.; Cooper, D. L.; Deegan, M. J. O.; Dobbyn, A. J.; Eckert, F.; Goll, E.; Hampel, C.; Hesselmann, A.; Hetzer, G.; Hrenar, T.; Jansen, G.; Köppl, C.; Liu, Y.; Lloyd, A. W.; Mata, R. A.; May, A. J.; McNicholas, S. J.; Meyer, W.; Mura, M. E.; Nicklass, A.; O'Neill, D. P.; Palmieri, P.; Peng, D.; Pflüger, K.; Pitzer, R.; Reiher, M.; Shiozaki, T.; Stoll, H.; Stone, A. J.; Tarroni, R.; Thorsteinsson, T.; Wang, M. see http://www.molpro.net

(14)(a) Schmidt, M. W.; Baldridge, K. K.; Boatz, J. A.; Elbert, S. T.; Gordon, M. S.; Jensen, J. H.; Koseki, S.; Matsunaga, N.; Nguyen, K. A.; Su, S.; Windus, T. L.; Dupuis, M.; Montgomery, J. A. *J. Comput. Chem.* **1993**, *14*, 1347

(14)(b) Gordon, M. S.; Schmidt, M. W. *Elsevier*, *Amsterdam.* **2005**, *41*, 1167

(15) Oosterom, V. A; Strackee, J. *IEEE Trans. Biom. Eng*. **1983**, BME-30(2): 125

(16) Gutsev, G. L.; Bartlett, R. J.; *Pol. J. of Chem.* **1998**, *72*, 1604

(17) Grant, D. J.; Dixon, D. A.; Camaioni, D.; Potter, R. G.; Christe, C. O. *Inorg. Chem.* **2009**, *48 (18)*, 8811

(18) Salem, L.; *Angew. Chem., Int. Ed. Engl.* **1972**, *11*, 92

(19) Jung, Y.; Head-Gordon, M. *ChemPhysChem*. **2003**, *4*, 522

(20) Kamada, K.; Ohta, K.; Shimizu, A.; Kubo, T.; Kishi, R.; Takahashi, H.; Botek, E.; Champagne, B; Nakano, M. *J. Phys. Chem. Lett.* **2010**, *1*, 937